Journal of Environmental Management xxx (xxxx) 114373

Contents lists available at ScienceDirect

Journal of Environmental Management

journal homepage: www.elsevier.com/locate/jenvman

Monitoring post-fire neighborhood competition effects on pine saplings under different environmental conditions by means of UAV multispectral data and structure-from-motion photogrammetry

José Manuel Fernández-Guisuraga [a,*], Leonor Calvo [a], Susana Suárez-Seoane [b]

[a] Area of Ecology, Faculty of Biological and Environmental Sciences, University of León, 24071,León, Spain
[b] Department of Organisms and Systems Biology (Ecology Unit) and Research Unit of Biodiversity (UO-CSIC-PA), University of Oviedo, Oviedo, Mieres, Spain

ARTICLE INFO

Keywords:
Competition
Fire
Object-based image analysis
Pine
Shrub
Unmanned aerial vehicle

ABSTRACT

In burned landscapes, the recruitment success of the tree dominant species mainly depends on plant competition mechanisms operating at fine spatial scale, that may hinder resource availability during the former years after the disturbance. Data acquisition at very high spatial resolution from unmanned aerial vehicles (UAV) have promoted new opportunities for understanding context-dependent competition processes in post-fire environments. Here, we explored the potentiality of UAV-borne data for assessing inter-specific competition effects of understory woody vegetation on pine saplings, as well as intra-specific interactions of neighboring saplings, across three burned landscapes located along a climatic/productivity gradient in the Iberian Peninsula. Geographic object-based image analysis (GEOBIA), including multiresolution segmentation and support vector machine (SVM) classification, was used to map pine saplings and understory shrubs at species level. Input data were, on the one hand, multispectral (11.31 cm·pixel^{-1}) and Structure-from-Motion (SfM) canopy height model (CHM) data fusion, hereafter MS-CHM, and, on the other, RGB (3.29 cm·pixel^{-1}) and CHM data fusion, hereafter RGB-CHM. A Random Forest (RF) regression algorithm was used to evaluate the effects of neighborhood competition on the relative growth in height of 50 pine saplings randomly sampled across the MS-CHM classified map. Circular plots of 3 m radius were set from the centroid of each target pine sapling to measure percentage cover, mean height of all individuals in the plot and mean height of individuals contacting the target sapling. Competing shrub species were differentiated according to their fire-adaptive traits (i.e. seeders *vs* resprouters). Object-based image classification applied on MS-CHM yielded higher overall accuracy for the three sites (83.67% ± 3.06%) than RGB-CHM (74.33% ± 3.21%). Intra-specific competitive effects were not detected, whereas increasing cover and height of shrub neighbors had a significant non-linear impact on the growth on pine saplings across the study sites. The strongest competitive effects of seeder shrubs occurred in open areas with low vegetation cover and fuel continuity, following a gap-dependent model. The non-linear relationships evidenced in this study between the structure of neighboring shrubs and the growth of pine seedlings/saplings have profound implications for considering possible competing thresholds in post-fire decision-making processes. These results endorse the use of UAV multispectral and SfM photogrammetry as a valuable post-fire management tool for measuring accurately the effect of competition in heterogeneous burned landscapes.

1. Introduction

Wildfires are one of the key processes determining the current landscape of the western Mediterranean Basin (Keeley et al., 2012; Arnan et al., 2013; Fernandes, 2013), strongly driving the composition, structure and dynamics of vegetation communities (Calvo et al., 2008; Taboada et al., 2017; Sagra et al., 2018). Under natural fire disturbance regimes, the resilience of Mediterranean communities is favored by fire-adaptive traits (e.g. vegetative resprouting, seeders reproductive precocity, serotiny and heat-shock triggered germination) acquired by plant species as a result of different evolutionary pathways (Keeley et al., 2011; Seidl et al., 2014; Keeley and Pausas, 2019; Chergui et al., 2020; Moya et al., 2021). Current shifts in natural fire regime parameters (mainly fire recurrence and severity) linked to both land use changes (Pausas, 2004) and anthropogenic climate warming (Vilà-Cabrera et al., 2018) have the potential to hinder ecological resilience (Turetsky et

* Corresponding author.
E-mail address: jofeg@unileon.es (J.M. Fernández-Guisuraga).

https://doi.org/10.1016/j.jenvman.2021.114373
Received 7 September 2021; Received in revised form 18 November 2021; Accepted 19 December 2021
0301-4797/© 2021

al., 2017; Keeley and Pausas, 2019; Moya et al., 2019; Fernández-Guisuraga et al., 2020a) and induce changes in plant dominance (Taboada et al., 2017).

Pine ecosystems dominated by *Pinus pinaster* Ait. and *Pinus halepensis* Mill., the most widely distributed pine forests in Mediterranean lowlands (Tapias et al., 2004), are particularly prone to stand-replacement fire events (Fernandes et al., 2008; Fernández-García et al., 2019). Both species are obligate seeders (Calvo et al., 2008; Pausas et al., 2008; Moya et al., 2018) that rely on the canopy seed bank inside serotinous cones to regenerate (Tapias et al., 2001, 2004), although the serotiny degree is highly fluctuating among individuals and populations (Tapias et al., 2001; Pausas et al., 2008). In this context, the increase of fire recurrence and burn severity can induce both failure of seedling recruitment because of immaturity risk (Calvo et al., 2008, 2016; Pausas et al., 2008) and high seedling mortality (Broncano and Retana, 2004; Fernandes et al., 2008), respectively. Likewise, pine seedling establishment and seedling/sapling growth may be upset (both positively and negatively) by shifts in the structure and composition of the woody understory community (Calvo et al., 2008; Fernández-García et al., 2019). Open spaces created after high severity stand-replacing fires can be readily re-occupied by resprouter species already present in the understory before the fire event (Calvo et al., 2003; Vivian and Cary, 2012). Additionally, recently burned areas could be quickly colonized by obligate seeders shrubs with fire-stimulated recruitment from existing seed banks (Taboada et al., 2017) or by opportunistic species that rely on seed dispersal from neighboring unburned patches (Arnan et al., 2013).

Inter-specific competitive effects of understory shrub species with fast recovery rate, as well as intra-specific effects of pine species with high recruitment rate, are expected to constrain the development of pine saplings at early post-fire stages (De las Heras et al., 2002; Calvo et al., 2008; Maia et al., 2012). This competitive process involves spatio-temporal changes in resource allocation (mainly space, nutrients, water and light; e.g. De las Heras et al., 2002; Calvo et al., 2008; Fernández-García et al., 2019), affecting the growth and physiology of pine saplings (Parker et al., 2010; de Oliveira et al., 2021). Furthermore, the effect of these competitive interactions on sapling's growth response is strongly associated with the composition, in terms of plant functional types, of the understory (Zhao et al., 2006; Parker et al., 2010; Metz et al., 2013). Nonetheless, facilitation mechanisms between pine saplings and understory shrubby vegetation, acting as nurse shrubs, have also been reported (Rodríguez-García et al., 2011a; Fernandes et al., 2017; Vaz et al., 2019) at short term after fire and under drought stress. These facilitation interactions can be turned into competition in later stages, when pine saplings outweigh the shrub layer and interfere with light interception (Eshel et al., 2000; Rodríguez-García et al., 2011a).

In most cases, post-fire management measures are essential to minimize competitive effects and ensure pine sapling performance after recurrent and severe wildfires (Taboada et al., 2017). Therefore, in-depth knowledge of plant inter-specific competition effects must be translated into reliable tools for supporting management decision-making in such scenarios (Zhao et al., 2006; Rodríguez-García et al., 2011b; Calama et al., 2019). Several field-based studies have identified the underlying processes of the inter and intra-specific competitive mechanisms of understory woody vegetation and neighboring pine saplings in post-fire landscapes dominated by *Pinus pinaster* and *Pinus halepensis* (e.g. De las Heras et al., 2002; Calvo et al., 2008; Taboada et al., 2017; Fernández-García et al., 2019). Although field work methods are highly accurate for this purpose, they often involve labor-intensive and time-consuming measurements (Metz et al., 2013; Versace et al., 2019a; Vanderwel et al., 2020). Therefore, accurate and reliable estimations of plant competitive interactions for quick applications at large scale have become a concern that must be addressed (Ma et al., 2017). In this sense, remote sensing-based approaches can overcome the limitations exhibited by methods based exclusively on ground measurements. Conventionally, light detection and ranging (LiDAR) active remote sensing data have been used to delineate three-dimensional forest canopy structure and crown structure of individual trees for quantifying intra and inter-specific competition in mature forest stands without the need of field data collection (e.g. Lo and Lin, 2013; Martin-Ducup et al., 2016; Ma et al., 2017; Versace et al., 2019b). Despite the accuracy of LiDAR data for estimating forest structure (Ma et al., 2017), the high monetary costs involved in such data acquisition restricts their use for researchers over large areas if data are not available through national plans (Getzin et al., 2014; Vanderwel et al., 2020). Additionally, multispectral passive remote sensing data acquired from satellite platforms, including high spatial resolution imagery, have been widely used to map species distribution and vegetation dynamics (Xie et al., 2008; Liang et al., 2020). However, measurements of ecosystem vertical structure using passive optical sensors is limited to secondary correlations between the reflectance signal and several top of canopy traits such as shadowing or moisture content (Healey et al., 2020; Fernández-Guisuraga et al., 2021a). Likewise, potential scale-gaps may exist between satellite data, even at high spatial resolution, and ground-based observations in heterogeneous ecological systems (Assmann et al., 2020). For their part, aerial surveys using manned aircrafts can deliver imagery at increased resolution than satellite missions (Cruzan et al., 2016) but it is usually not high enough to estimate the distribution of individual plant species in heterogeneous ecological systems (Turner et al., 2011; Whitehead and Hugenholtz, 2014) and the costs regarding aircraft hire, mobilization and personnel are very high (>$1000 US per survey hour; Colefax et al., 2018) for most ecological research needs and management actions (Anderson and Gaston, 2013; Cruzan et al., 2016) and they pose difficult campaign organization efforts (Matese et al., 2015).

In recent years, unmanned aerial vehicles (UAVs) represent a suitable alternative for measuring ecological processes by the acquisition of very high spatial resolution data on-demand without cloud contamination, derived from their very low-altitude flight capability (Anderson and Gaston, 2013), and at a much lower cost than manned aircrafts surveys carrying multispectral or LiDAR sensors (Vanderwel et al., 2020). The good maneuverability of UAVs due to their low flying speed, which cannot be achieved by manned aircrafts (Baxter and Hamilton, 2018), is key for surveying complex environments (Whitehead and Hugenholtz, 2014) and relates to increased product geospatial accuracy and survey repeatability (Watts et al., 2010). Besides being able to produce orthomosaics of the region of interest through RGB, multispectral (MS) or hyperspectral (HS) orthorectified images collected by on-board UAV sensors (Deng et al., 2018), 3-D point clouds (height data) can be also derived from UAV imagery by a Structure-from-Motion (SfM) photogrammetry workflow (Komárek et al., 2018; Carabassa et al., 2020) to estimate co-registered spectral and structural traits of vegetation canopies (Dandois et al., 2015). Recently, LiDAR sensors on-board UAV platforms have been used to monitor forest structure, providing more accurate vertical data than SfM (Wallace et al., 2016). However, the costs of LiDAR sensor plus a suitable UAV platform remain high compared to RGB and MS cameras (Prošek and Šímová, 2019). Overall, the technical maturity of UAVs and SfM photogrammetry workflows applied to the imagery captured by on-board sensors, represent two consumer-grade technologies that offer new opportunities for capturing scale-appropriate vegetation structural data not possible or functional with other remote sensing techniques (Anderson and Gaston, 2013; Dandois et al., 2015).

Geographic Object-Based Image Analysis (GEOBIA) has proven to yield better results than traditional pixel-based approaches when processing remote sensing data at very high spatial resolution (e.g. Blaschke, 2010; Myint et al., 2011; Whiteside et al., 2011) due to the following particularities of UAV-borne data: (i) low signal-to-noise ratio (Lourenço et al., 2021) and (ii) high amount of shadows owing to the large parallax effect considering the low flight altitude of the surveys (Modica et al., 2020). Despite the major advantages of SfM photogrammetry applied to UAV imagery on the assessment of different ecological processes, the spatial monitoring of plant competitive interactions at species level in post-fire landscapes has not been addressed yet. In this sense, UAV imagery would provide scale-appropriate data to capture vegetation competitive effects in Mediterranean burned landscapes that exhibit a high spatial heterogeneity arising from the fine-grained arrangement of vegetation legacies and filter effects from environmental conditions (Fang et al., 2019; Walker et al., 2019). For instance, Vanderwel et al. (2020) used UAV-borne data to measure neighborhood crowding of two species in a mature forest stand in western Canada with promising results. However, to the best of our knowledge, no study has applied this technology in recently burned landscapes, where vegetation mapping of fine-grained mosaics of heterogeneous shrub composition remains challenging (Prošek and Šímová, 2019).

To address this knowledge gap, we performed UAV surveys along an Atlantic-Transition-Mediterranean climatic gradient in the Iberian Peninsula within the perimeter of three burned landscapes dominated by *Pinus pinaster* and *Pinus halepensis*. In this context, we explored the potentiality of UAV-borne data at very high spatial resolution (RGB and MS orthomosaics, as well as a canopy height models -CHM-) to map the distribution and structural properties of pine saplings and understory shrubs at species level four years after fire, by means of GEOBIA, and evaluate from that properties the intra and inter-specific competition effects on pine saplings under different environmental conditions. Specifically, we sought to address the following questions: (i) Do the RGB, MS and height products derived from UAV data provide enough accuracy for species level classification and estimation of structural properties at species level in recently burned landscapes? (ii) Is the development of pine saplings conditioned by inter-specific competitive effects of neighboring shrub understory species and by intra-specific competition of neighboring pine saplings? (iii) Do the shrub competitive effects differ according to their fire-adaptive traits and are these competition patterns maintained throughout different environmental conditions?

We expect: (i) The centimeter resolution of UAV products would be appropriate for capturing the fine-grained arrangement of vegetation patches in the evaluated post-fire landscapes (Fernández-Guisuraga et al., 2018; Walker et al., 2019). (ii) The spectral information captured by MS sensors would provide better performance than RGB sensors at species level classification, despite the lower spatial resolution of the former (Komárek et al., 2018). (iii) The shrub understory species and neighboring saplings would exert negative effects on the growth of pine saplings, the competition being more intense the higher are neighbor individuals. Since *Pinus pinaster* and *Pinus halepensis* saplings are heliophiles (Richardson, 2000), they would be negatively affected by tall neighbors that could reduce the amount of light (Calvo et al., 2008; Vanderwel et al., 2020). (iv) Competitive effects of resprouter shrubs would be more pronounced in productive environments (Pausas and Keeley, 2014) given the ability of that species to regenerate rapidly after the wildfire (Calvo et al., 2003; Taboada et al., 2017).

2. Material and methods

2.1. Study sites

Three burned sites located along an Atlantic-Transition-Mediterranean climatic and productivity gradient on a northwest-southeast axis of the Iberian Peninsula (Fig. 1) were selected.

The Atlantic site is located within a burned scar of 2,523ha of a stand-replacing wildfire that predominantly affected a *Pinus pinaster* stand in September of 2013. The altitude ranges between 0 and 628 m above sea level (ASL). The climate of the region is Atlantic (Fernández-Guisuraga et al., 2019a), with mean annual temperature of 13 °C, mean annual precipitation of 1655 mm and absence of summer drought (Ninyerola et al., 2005). Soils are acidic and mostly classified as Umbrisols (Jones et al., 2005). Vegetation cover four years after the wildfire mainly consisted of tree regeneration stands of *Pinus pinaster* in a seedling and sapling growth stage and resprouting stands of *Eucalyptus*

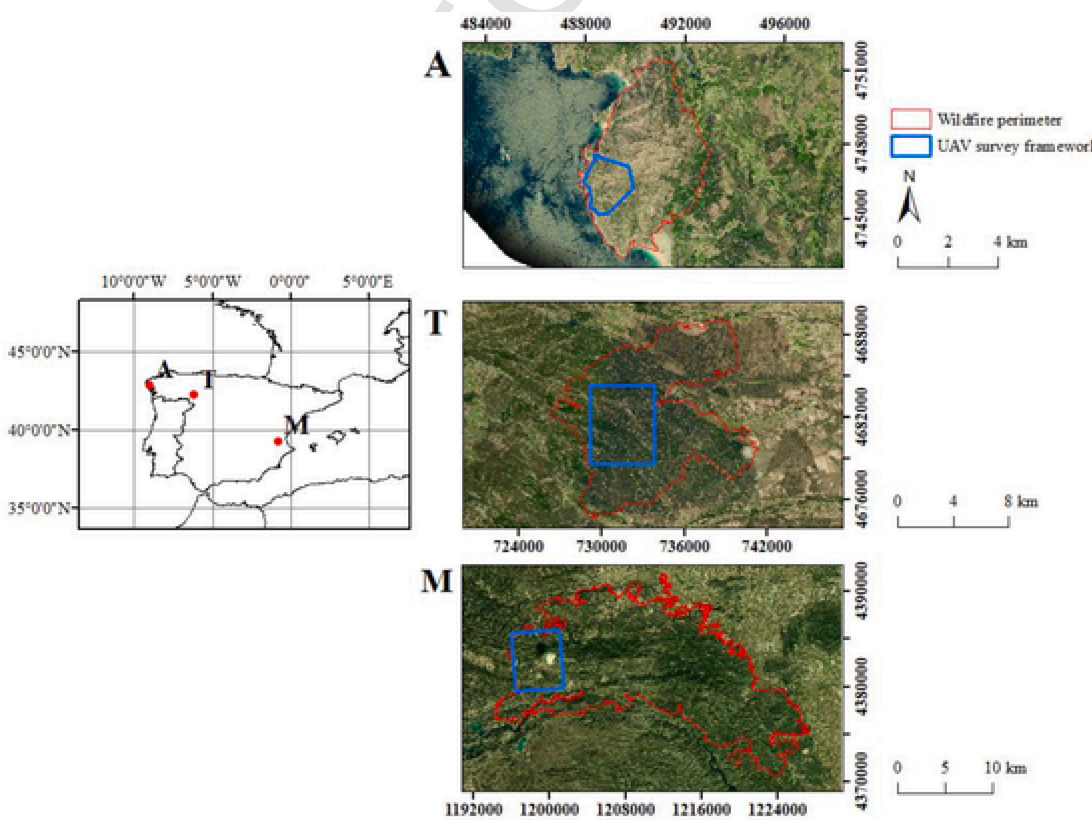

Fig. 1. Location of the Atlantic (A), Transition (T) and Mediterranean (M) study sites along a west-east climatic gradient in the Iberian Peninsula.

globulus Labill. The shrub community is dominated by *Cytisus scoparius* (L.) Link, *Erica australis* L., *Rubus* L. sp. and *Ulex europaeus* L.

The Transition site is located within the perimeter of a convective crown stand-replacing wildfire that burned 11,602ha in August 2012, predominantly covered by a *Pinus pinaster* stand. The study site lies at an altitudinal range of 836–1499 m ASL. The climate corresponds to a Mediterranean transition area (Fernández-Guisuraga et al., 2019a), with a mean annual temperature of 10 °C, a mean precipitation of 640 mm and less than two months of summer drought (Ninyerola et al., 2005). The soils are predominantly acidic and classified as Haplic Umbrisol and Dystric Regosol (Jones et al., 2005). Four years after the wildfire, vegetation was dominated by mature *Quercus pyrenaica* Willd. tree stands and *Pinus pinaster* regeneration stands in a seedling or sapling growth stage. The predominant shrub species are *Erica australis*, *Halimium lasianthum* subsp. *alyssoides* (Lam.) and *Pterospartum tridentatum* (L.) Willk.

The Mediterranean site lies within the perimeter of a convective crown stand-replacing wildfire occurred in June 2012, which burned 29,752ha of mature *Pinus halepensis* tree stand, as well as a large extension of a shrub community dominated mainly by *Cistus* L. sp., *Quercus coccifera* L., *Rosmarinus officinalis* L. and *Ulex parviflorus* Pourr. The altitude of the site ranges between 114 and 995 m ASL. The climate is Mediterranean (Fernández-Guisuraga et al., 2019a), with a mean annual temperature and precipitation of 16 °C and 582 mm, respectively, and three months of summer drought (Ninyerola et al., 2005). Soils are basic and classified as Haplic Calcisol and Lithic Leptosol (Jones et al., 2005). Vegetation cover was dominated four years after the wildfire by the above-mentioned pre-fire species.

2.2. UAV platform and sensor

Aerial surveys were performed with an FV8 octorotor (ATyges, Málaga, Spain) (Fig. 2). This platform weighs 3.5 kg and supports a maximum payload of 1.5 kg. The eight brushless motors are powered by two 8200 mAh lithium-ion batteries, ensuring an operational time of at least 20 min. The flight controller is an ATmega 1284 P (Microchip Technology Inc., Chandler, AZ, USA), being the navigation control board based on an Atmel ARM9 microcontroller. A LEA-6 (u-blox, Thalwil, Switzerland) was selected as GPS module. The UAV platform was controlled by a 12-channel MZ-24 HoTT radio transmitter (Graupner, Kirchheim unter Teck, Germany) operating at 2.4 GHz. See Fernández-Guisuraga et al. (2018) for more technical details.

The Parrot Sequoia camera (Parrot SA, Paris, France) was mounted underneath the UAV platform using a gimbal stabilizer. The camera comprises: (i) a MS sensor which collect data along four broadband bands in the visible and NIR spectral regions (Table 1A) using global shutter; (ii) a RGB sensor (Table 1B) using rolling shutter (Parrot, 2020).

MS and RGB sensor specifications (Table 1) ensured a ground sample distance (GSD) of 11.31 cm·pixel^{-1} and 3.29 cm·pixel^{-1}, respectively, with a flight altitude of 120 m above ground level (AGL). The camera was bundled with an irradiance sensor to record light conditions in the same spectral bands as the MS sensor during the survey in order to correct the signal captured by the sensor in both clear and overcast conditions (Deng et al., 2018). The weight of the MS camera is 72 g and that of the irradiance sensor 35 g. Raw images are captured in a 16-bit format. Camera ISO value and exposure time was set to automatic. Image capture settings and light data collected by the irradiance sensor are stored as input metadata in the photogrammetry data processing.

Fig. 2. UAV platform (ATyges FV8) used in the surveys.

Table 1
Parrot Sequoia camera specifications.

A) Multispectral sensor			
Image resolution	1.2 MP (1,280 × 960p)		
Focal length (mm)	3.98		
Sensor width (mm)	4.80		
Field of view (º)	HFOV	VFOV	DFOV
	62	49	74
Band configuration	# Band	Band center (nm)	Band width (nm)
	B1 (green)	550	40
	B2 (red)	660	40
	B3 (red edge)	735	10
	B4 (NIR)	790	40
B) RGB sensor			
Image resolution	16 MP (4,608 × 3, 456p)		
Focal length (mm)	4.88		
Sensor width (mm)	6.17		
Field of view	HFOV (º)	VFOV (º)	DFOV (º)
	64	50	74

2.3. UAV survey

The UAV survey campaign was conducted four years after the wildfire in each study site during the biomass peak (i.e. between June and July 2016 in the Transition site, in August 2016 in the Mediterranean site and June 2017 in the Atlantic site). The extension of the survey frameworks was 300ha, 2,700ha and 3,000ha respectively for the Atlantic, Transition and Mediterranean sites (Fig. 1). These frameworks were located in areas highly dominated by pine stands in the pre-fire situation. Given the large area of the survey frameworks, the flights were performed within a 6-h window around the solar midday. Severe overcast time intervals were avoided, although small variations in illumination conditions were corrected at the beginning of the photogrammetry data processing using the data collected with the irradiance sensor. All the flights were scheduled with Mikrokopter Tools software keeping a constant flight height of 120 m AGL in terrain following mode using a digital terrain model (DTM) at 5 m of spatial resolution from the Spanish Aerial Ortho-photography National Plan (PNOA). The average cruise speed was 10 m s^{-1}. The camera trigger distance was set to 22.4 m, achieving and along-track overlap of 80%. The cross-track overlap was also set to 80%. An overlap of a flight line was established between adjacent flights. An Airinov radiometric calibration target was recorded with the MS sensor before each flight to perform radiometric calibration of the MS imagery in the photogrammetry processing stage. Accounting for MS and RGB imagery, around 24,000 raw images were acquired in the Atlantic site, 230,000 in the Transition site and 168,000 in the Mediterranean site, representing approximately 1 TB of raw data.

2.4. Photogrammetry data pre-processing

UAV data processing was implemented in Agisoft Metashape 1.6 (Agisoft LLC, St. Petersburg, Russia), a Structure-from-Motion (SfM) and photogrammetry software whose workflow includes four main stages (Deng et al., 2018; Agisoft, 2019; Prošek and Šímová, 2019): (i) camera alignment in which each camera position and external orientation is estimated, building a sparse point cloud model; (ii) surface reconstruction through a dense point cloud generation based on the estimated camera positions; (iii) generation of a digital elevation model (DEM) surface by means of grid interpolation of the densified point cloud; and (iv) image orthorectification and orthomosaic generation based on image external orientation and DEM surface. Before the processing workflow, MS imagery of each flight was calibrated radiometrically using the irradiance sensor metadata and the radiometric calibration target to obtain an absolute reflectance product. The SfM project of each study site was split into ten chunks after camera alignment step to overcome the processing limits of large UAV datasets. The parameters used in the SfM workflow are summarized in Table 2. External camera orientation was improved using at least ten ground control points (GCPs) evenly distributed per chunk. GCPs were extracted from aerial orthophotos of the PNOA, with a GSD of 10 cm and planimetric and altimetric accuracies of $RMSE_{X,Y} < 0.50$ m and $RMSE_Z < 1$ m, respectively. At the end of the SfM workflow, we obtained for the three study sites: (i) a MS orthomosaic calibrated to absolute reflectance with a GSD of 11.31 cm·pixel^{-1}; (ii) a RGB orthomosaic with a GSD of 3.29 cm·pixel^{-1}; (iii) a DEM with a GSD of 6.58 cm·pixel^{-1}; and (iv) a canopy height model (CHM) with a GSD of 6.58 cm·pixel^{-1} computed by subtracting the UAV digital terrain model (UAV-DTM) from the DEM. The UAV-DTM was derived by classifying the dense point cloud into ground points and non-ground points. We used the parameters value proposed by Prošek and Šímová (2019) to successfully classify the dense point cloud (max angle = 10°, max distance 0.2 m and cell size = 5 m) given the similarity in topography and vegetation structure between their study area and ours.

2.5. Field sampling

We conducted a field sampling campaign contemporary to UAV survey in each study site (i.e. between June and July 2016 in the Transition site, in August 2016 in the Mediterranean site and in June 2017 in the Atlantic site) to collect vegetation ground truth data for training (60% of the data) and validating (40% of the data) the classification algorithm. Presence data for each plant species (pine saplings and shrub species) were obtained in homogeneous plots of 2 m × 2 m, randomly established in the field. Each plot was representative for a plant species, in terms of the highest possible dominance of the species of interest and avoiding species superposition. The center of each plot was georeferenced with a sub-meter accuracy GPS receiver in post-processing mode. Non-interest classes (e.g. rocks or man-made surfaces) were sampled using the RGB orthomosaic of each study site. The number of plots was stratified considering the approximate surface occupied by each plant species within the study sites under expert field knowledge, with a minimum of thirty samples per class. Shrub species were classified according to their main fire-adaptive trait (seeders and resprouters) from field observations in the study sites (Table 3). In addition to presence data, the mean height and cover of pine saplings and shrub species grouped by their fire-adaptive traits were measured in the validation plots to perform accuracy evaluation of the UAV estimates of these variables obtained in subsequent analyses to be used in competition assessment. Cover variables were estimated using a visual estimation method (Fernández-Guisuraga et al., 2021b). The coefficient of determination (R^2) and root-mean-squared error (RMSE) from linear regression were computed to quantify the agreement between the UAV-derived estimations and field data.

2.6. Orthomosaic segmentation and classification

Geographic Object-Based Image Analysis (GEOBIA) approach was used to define representative image objects (i.e. non-overlapping clusters of neighboring pixels that represent the same ground feature; Modica et al., 2020) through image segmentation based on spectral and spatial information, and implement subsequently an object-based image classification to map vegetation at genus or species level in the three study sites. Image segmentation and object-based classification using as inputs: (i) the MS orthomosaic (green, red, red edge and NIR bands) together with the CHM, hereafter MS-CHM, and (ii) the RGB orthomosaic (red, green and blue channels) together with the CHM, hereafter RGB-CHM, was conducted in eCognition 9 software (Trimble Inc., Sunnyvale, United States).

We used multiresolution segmentation (MRS; Baatz and Schäpe, 2000), one of the most successful and widely used segmentation algorithms (Witharana and Civco, 2014) in remote sensing applications using very high spatial resolution imagery in recent studies (e.g. Drăguţ et al., 2014; Liu et al., 2015; Li et al., 2016; Nuijten et al., 2019; Prošek and Šímová, 2019; Daryaei et al., 2020; Lourenço et al., 2021). MRS is a region-based technique, in a bottom-up or region-growing approach, based on the iterative fusion of neighboring into image objects if a homogeneity criterion is satisfied (Duro et al., 2012; Belgiu and Csillik, 2018; Lourenço et al., 2021). This criterion is controlled through three parameter settings defined by the user: scale, shape and compactness (Table 4). The scale parameter controls the relative size of the image objects, usually in a direct relationship (Duro et al., 2012). Thus, scale is considered the most important MRS parameter since the size of the objects has a great impact on the classification accuracy (Smith, 2010; Myint et al., 2011; Drăguţ et al., 2014; Witharana and Civco, 2014; Modica et al., 2020). Finding optimal scale parameter values is conducted through trial-and-error processes (e.g. Duro et al., 2012; Prošek and Šímová, 2019), as well as supervised (e.g. Smith and Morton, 2010; Liu et al., 2012) and unsupervised methods (e.g. Zhang et al., 2008;

Table 2
Parameter settings in the Structure-from-Motion (SfM) workflow.

SfM workflow step	Parameter	Setting
camera alignment	accuracy	high
	generic preselection	yes
	reference preselection	yes
	key point limit	40,000
	tie point limit	4000
dense point cloud generation	quality	high
	depth filtering	aggressive
DEM generation	source data	dense cloud
	interpolation	enabled
orthomosaic generation	surface	DEM
	blending mode	mosaic
	hole filling	yes

Table 3
Vegetation ground truth data sampled in the field sampling campaign of each study site and fire-adaptive traits of each shrub species.

Site	Species	Fire-adaptive trait	# of plots/samples
Atlantic	*Cytisus scoparius*	Seeder	34
	Erica sp.	Resprouter	41
	Eucalyptus globulus	Resprouter	30
	Pinus pinaster	Seeder	58
	Rubus sp.	Resprouter	33
	Ulex europaeus	Seeder	97
	Grassland	–	61
Transition	*Erica* sp.	Resprouter	45
	Halimium lasianthum	Seeder	64
	Pinus pinaster	Seeder	66
	Pterospartum tridentatum	Resprouter	40
	Grassland	–	51
Mediterranean	*Cistus* sp.	Seeder	39
	Pinus halepensis	Seeder	44
	Quercus coccifera	Resprouter	38
	Ulex parviflorus	Seeder	60
	Grassland	–	32

Table 4
Multiresolution segmentation (MRS) parameter values and summary of segmentation results in the Atlantic, Transition and Mediterranean sites.

Scale	Atlantic site	Transition site	Mediterranean site
level 2 (coarse scale)	100	70	100
# of objects	1.39×10^5	2.34×10^6	1.22×10^6
Mean object size	47.68 m^2	18.27 m^2	61.83 m^2
level 1 (fine scale)	20	20	30
# of objects	3.98×10^6	3.56×10^7	1.70×10^7
Mean object size	0.62 m^2	0.57 m^2	0.91 m^2
Shape	0.3	0.3	0.3
Compactness	0.5	0.5	0.5

Drăguţ et al., 2010; Drăguţ et al., 2014). Among these methods, unsupervised approaches are the most robust, rigorous and reproducible (Witharana and Civco, 2014). We used the estimation of scale parameter (ESP2) unsupervised tool proposed by Drăguţ et al. (2014), together with visual interpretation of the segmentation results and expert knowledge. ESP2 is based on the calculation of local variance on each input imagery band to find the appropriate scale parameter regarding the observed ground structures in a three-level hierarchy approach. ESP2 iterations to find the optimal scales in each study site were conducted in small representative areas of the MS and RGB orthomosaics given the large extent of the scenes. MRS shape parameter was set to 0.3 to assign more weight on the spectral variability than shape for image segmentation, whereas the compactness parameter was set to 0.5 to equally account for object compactness and smoothness (Myint et al., 2011; Whiteside et al., 2011). We assigned the same weight to each band of the RGB orthomosaic and the CHM in the MRS approach. A double weight was assigned for the red edge and NIR bands of the MS orthomosaic given the relevance of the vegetation signal in these regions of the spectrum (Fernández-Guisuraga et al., 2019b).

Two scale levels (coarse and fine) were chosen for the three study sites. The coarse segmentation scale (i.e. level 2) allowed to delineate objects that comprise ground covers occurring in large patches, such as *Eucalyptus globulus* stands in the Atlantic site. However, objects comprising shrub vegetation patches at this scale would sometimes have a noticeable spectral variability as a result of the presence of different species. Since the objective of this GEOBIA approach is to classify ground cover at the species level, the finer segmentation scale (i.e. level 1) allowed to delineate objects that largely correspond to small patches occupied by individuals of each shrub species. The multilevel image segmentation approach has proven to improve the classification accuracy in GEOBIA approach (e.g. Myint et al., 2011; Whiteside et al., 2011; Duro et al., 2012).

Support Vector Machine (SVM) algorithm was used to classify multiscale segmented objects from the MS-CHM and RGB-CHM into the considered ground cover classes for each study site (Table 3). SVM is a nonparametric supervised learning technique (Cortes and Vapnik, 1995) widely used in UAV vegetation mapping field (e.g. Müllerová et al., 2017; Komárek et al., 2018; Vasantha and Keesara, 2020). SVM often provides higher classification accuracy than traditional classifiers, achieves better generalization and performs efficiently even with small training data sets (Mountrakis et al., 2011). We used as inputs to the SVM classifier several features computed from the pixel values of each band within the segmented objects (min-max, mean and standard deviation), Haralick co-occurrence texture measures (Haralick et al., 1973) within each object (mean, standard deviation, contrast, correlation, entropy and homogeneity) and object shape features (asymmetry, compactness, roundness). Texture features were selected based on previous research in the study sites (Fernández-Guisuraga et al., 2019a, 2019b). For the selection of remaining object features, we relied on expert knowledge with conducting GEOBIA analysis in burned landscapes. After repeated experiments in the study sites, a radial basis function (RBF) kernel with penalty parameter (C) equal to 100 and gamma parameter (γ) equal to 0.2 were used in SVM configuration. Indeed, Yang (2011) evidenced the robustness of RBF kernel when classifying spectrally heterogeneous ground cover.

Ground truth data was randomly split into training (60%) and validation (40%) subsets for the SVM classifier. From the confusion matrix of the classification, we computed several accuracy metrics: overall accuracy, Kappa index and user's and producer's accuracy of each class. Based on accuracy results, the subsequent analyses were performed using the best classified UAV product (MS-CHM or RGB-CHM inputs) at genus or species level for each study site.

2.7. Neighborhood competition analysis

The effect of vegetation neighborhood competition on pine saplings was evaluated, separately for each study site, using Random Forest (RF) regression (Breiman, 2001). RF is an ensemble learning algorithm based on classification and regression trees (CART; Oliveira et al., 2012). The algorithm fits multiple CARTs through bootstrap aggregating techniques, which help to reduce overfitting issues and improve the stability and accuracy of the algorithm (Cutler et al., 2007). RF can also handle spatial autocorrelation in the predictors and complex non-linear relationships and interaction effects between predictors and dependent variables (García-Llamas et al., 2020). In each study site, the classified map was used to randomly sample 50 target pine saplings, separated at least 100 m. A distance of at least 5 m from the saplings to the forest edge was ensured following the criteria by Lanzer et al. (2017). The height of each target pine sapling was used as dependent variable in the RF algorithm, since the competitive effects on pine saplings four years after fire are mainly evident through changes in the relative growth in height (Calvo et al., 2008). Analysis of competing factors of shrub vegetation species grouped by their fire-adaptive traits (i.e. seeders and resprouters; Table 3) and neighboring pine saplings was undertaken within circular plots of 3 m radius from the centroid of each target pine sapling. The plot size was chosen on the basis of the maximum radius (approximately 1 m) of the pine saplings observed in the field and as suggested by Sánchez-Pinillos et al. (2018). Within each plot, the percentage cover, the mean height of all individuals in the plot and the mean height of individuals contacting the target sapling were measured at the level of shrub species grouped by resprouting and seeding strategy, and at the level of competing pines other than target saplings, as predictors of competing effects using the MS-CHM classified map and the CHM. These variables are commonly used in field-based research to assess competitive effects on pine saplings (O'Brien et al., 2007; Knapp et al., 2008; Rodríguez-García et al., 2011b; Taboada et al., 2017). Prior to RF models, a data exploration analysis was conducted to discard potential multicollinearity among the predictors through Bivariate Pearson correlations (Fernández-Guisuraga et al., 2020b). All predictors had low correlation coefficients ($r < |0.7|$) and were selected for further modelling (García-Llamas et al., 2020).

The variance explained (R^2) by the RF model in each study site was computed using the internal out-of-bag error rate. This approach avoids the use of an independent validation dataset (Cutler et al., 2007; García-Llamas et al., 2020). The model parameter *mtry* was set using tuning experiments to find the value with the minimum error estimate (Liaw and Wiener, 2002; Oliveira et al., 2012). Additionally, *ntree* parameter was set to the recommended value of 1000 in order to obtain stable predictions (Probst and Boulesteix, 2018). The relative importance of each predictor to the explained model variance was evaluated through the percentage increase in mean square error (%IncMSE). A parsimonious subset of the predictors was selected through a forward model selection routine proposed by Kane et al. (2015) to identify the key effects of competing vegetation on target pine saplings in each study site with a much clearer and simpler interpretation than using a full model including all the predictors regardless of their relative contribution. The effects of competing vegetation on pine sapling growth were examined through partial dependence plots.

RF regression models were implemented in R (R Core Team, 2020) using the 'RandomForest' package (Liaw and Wiener, 2002).

3. Results

The object-based image classification developed for the three study sites on the basis of the SVM algorithm featured higher overall accuracy using MS-CHM (83.67% ± 3.06%) than RGB-CHM (74.33% ± 3.21%) as input data. Consequently, the classified vegetation maps based on MS-CHM data were selected for the following analyses (see Fig. 3 for a detailed map view).

The highest classification accuracy was achieved in the Transition site (overall accuracy -OA- = 87% and Kappa = 0.83), followed by the Atlantic (OA = 83% and Kappa = 0.80) and Mediterranean (OA = 81% and Kappa = 0.76) sites. In general, producer's (PA) and user's (UA) accuracy of each shrub and pine sapling species were consistent with OA values in the three study sites. Therefore, it can be assumed that the classification error was evenly distributed between plant species. Specifically, PA and UA values were higher than 70% in all cases. Remarkably, *Pinus pinaster* and *Pinus halepensis* saplings were classified with PA and UA higher than 85% across sites. The least accurate results in the Atlantic site were registered for *Cytisus scoparius*, which was confused with *Ulex europaeus* in 29% of the cases. In the Transition site, species distribution was slightly under or overestimated (11% ± 2.5%). For their part, *Ulex parviflorus* and *Quercus coccifera* in the Mediterranean site were confused among them in up to 20% of the cases. (Table 5 and Figure SM1 of the Supplementary material).

Cover variables computed from the classified map were strongly associated with field measurements in the three study sites (R^2 > 0.86 and RMSE <6.36%). The UAV-derived canopy mean height was also successfully correlated with field data for both pine saplings and shrubs (R^2 > 0.70 and RMSE <28.24 cm) (Table 6). On the basis of the classified vegetation maps, the cover of pine saplings was lower than 5% in the three study sites. Shrub species with seed germination traits (Table 3) covered 36% of the surface in the Atlantic site, 37% in the Transition site and 32% in the Mediterranean site. For their part, the cover of resprouter shrub species (Table 3) was 30%, 38% and 12% in the Atlantic, Transition and Mediterranean sites, respectively.

The structure of neighboring shrub species successfully explained the target pine saplings relative growth in height in the Atlantic (R^2 = 0.74), Transition (R^2 = 0.75) and Mediterranean (R^2 = 0.82) burned sites through parsimonious RF models (Fig. 4). In the initial stage of the parsimonious model selection routine, the variance explained by the full model (i.e. including all the predictors) was substantially lower in the three sites (R^2 = 0.61 ± 0.07) (Table 7).

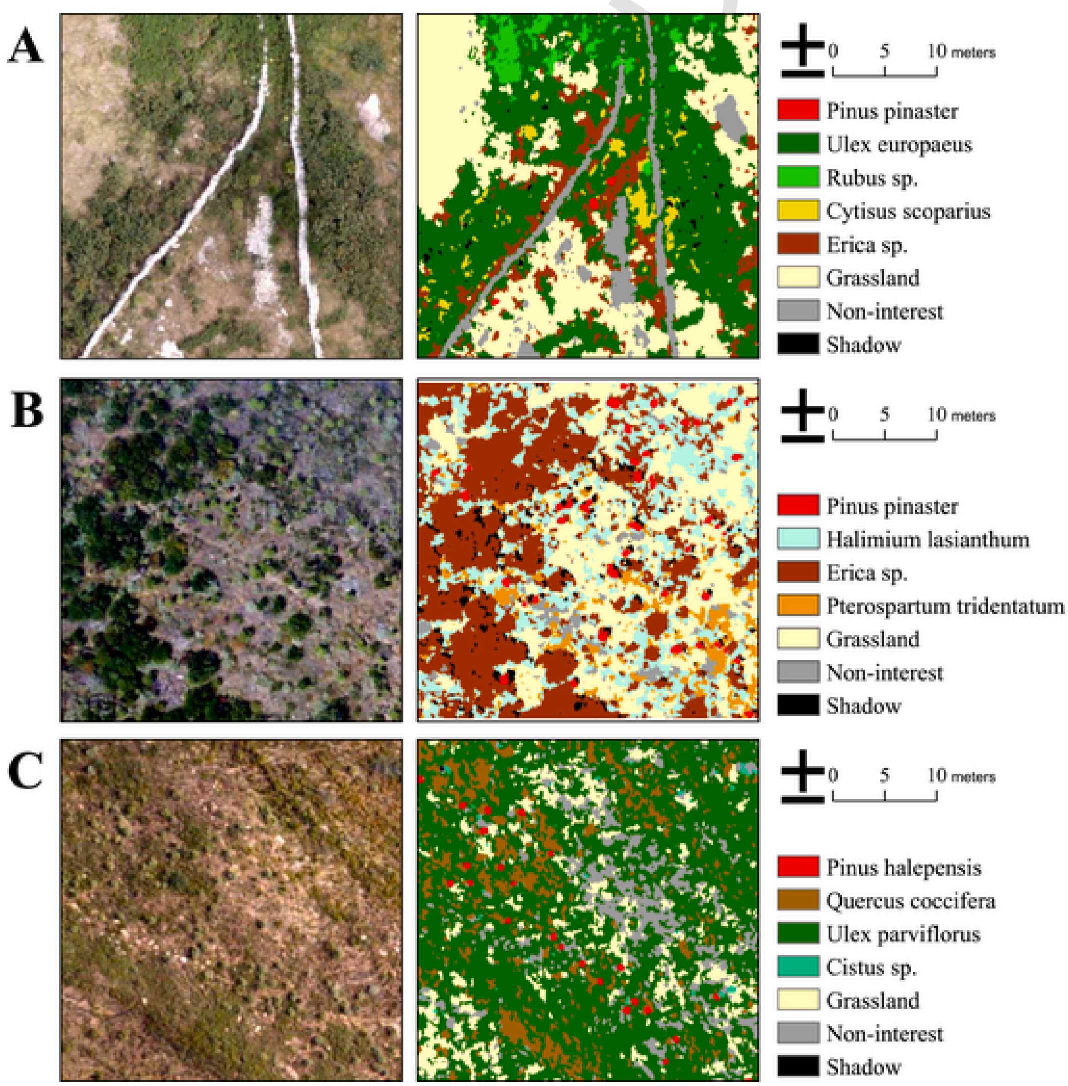

Fig. 3. Detailed view of the RGB orthomosaic (left) and the vegetation classified map (right) produced from multispectral and height data classification for complex areas in terms of ground cover heterogeneity with pine saplings presence in the Atlantic (A), Transition (B) and Mediterranean (C) study sites.

Table 5
Confusion matrix of the classification using multispectral UAV data, reporting the overall, producer's (PA) and user's (UA) accuracy, as well as the Kappa index. See Table SM1 of the Supplementary material for the confusion matrix of the classification scheme using RGB UAV data.

	ATLANTIC SITE	REFERENCE DATA						
		Cytisus scoparius	*Erica* sp.	*Eucalyptus globulus*	*Pinus pinaster*	*Rubus* sp.	*Ulex europaeus*	Grassland
CLASSIFIED DATA	*Cytisus scoparius*	10	1	0	0	0	3	0
	Erica sp.	2	13	0	0	0	2	0
	Eucalyptus globulus	0	0	10	0	1	0	0
	Pinus pinaster	2	0	0	20	0	1	1
	Rubus sp.	0	0	2	0	10	0	2
	Ulex europaeus	0	2	0	3	0	33	0
	Grassland	0	0	0	0	2	0	21
	producer's accuracy (%)	71	81	83	87	77	85	88
	user's accuracy (%)	71	76	91	85	71	87	91
	Overall accuracy (%)	**Kappa index**						
	83	80						
	TRANSITION SITE	REFERENCE DATA						
		Erica sp.	*Halimium lasianthum*	*Pinus pinaster*	*Pterospartum tridentatum*	Grassland		
CLASSIFIED DATA	*Erica* sp.	15	0	1	0	0		
	Halimium lasianthum	0	24	2	2	1		
	Pinus pinaster	1	0	22	0	0		
	Pterospartum tridentatum	2	0	0	12	0		
	Grassland	0	2	1	2	19		
	producer's accuracy (%)	83	92	85	75	95		
	user's accuracy (%)	94	83	96	86	79		
	Overall accuracy (%)	**Kappa index**						
	87	83						
	MEDITERRANEAN SITE	REFERENCE DATA						
		Cistus sp.	*Pinus halepensis*	*Quercus coccifera*	*Ulex parviflorus*	Grassland		
CLASSIFIED DATA	*Cistus* sp.	12	0	0	1	2		
	Pinus halepensis	1	16	0	0	0		
	Quercus coccifera	0	0	12	3	0		
	Ulex parviflorus	1	2	3	19	0		
	Grassland	2	0	0	1	11		
	producer's accuracy (%)	75	89	80	79	85		
	user's accuracy (%)	80	94	80	76	79		
	Overall accuracy (%)	**Kappa index**						
	81	76						

Table 6
Relationship between field-sampled and UAV-estimated cover and mean height of pine saplings, seeder shrubs and resprouter shrubs for the Atlantic, Transition and Mediterranean sites.

	Atlantic site		Transition site		Mediterranean site	
	R^2	RMSE	R^2	RMSE	R^2	RMSE
Pine saplings						
Cover (%)	0.86	6.18	0.92	5.98	0.87	6.36
Mean height (cm)	0.72	25.39	0.74	22.78	0.70	28.24
Seeder shrub species						
Cover (%)	0.93	5.44	0.94	5.87	0.95	5.86
Mean height (cm)	0.77	23.84	0.77	19.86	0.81	18.33
Resprouter shrub species						
Cover (%)	0.91	5.75	0.96	5.61	0.88	6.08
Mean height (cm)	0.74	21.99	0.80	17.79	0.76	23.21

The growth of *Pinus pinaster* and *Pinus halepensis* saplings was undermined by inter-specific competitive effects in neighborhoods with greater shrub species cover and height in the three study sites, being the relationships between shrubs (both seeders and resprouters) and pine sapling mostly non-linear. Nevertheless, intra-specific competitive effects were not observed at the light of the parsimonious RF models. The competition intensity of shrub species according to their fire-adaptive traits (i.e. seeders and resprouters) was site-dependent. Under Atlantic conditions, both the cover (>30%) and height of contacting individuals (>0.35 m) of seeder shrubs (mainly *Ulex europaeus*) impacted pine sapling height growth (Fig. 4A). The mean height of resprouter shrubs also had a significant effect on pine sapling height, but to a lesser extent and more gradually than seeders. In the Transition site, inter-specific competition effects of resprouters (*Erica* sp. and *Pterospartum tridentatum*) were more pronounced (IncMSE >26%) than those of seeders (IncMSE ≤10%) (Fig. 4B). The cover and height of contacting resprouters individuals, higher than 20% and 0.4 m, respectively, heavily affected pine sapling performance. Finally, in the Mediterranean site, only seeder shrubs (*Ulex parviflorus* and *Cistus* sp.) had competitive effects on pine saplings (Fig. 4C), being the strongest impact induced by contacting seeders taller than 0.5 m.

4. Discussion

The understanding of the context-dependent ecological competition processes is considered essential for supporting adequate management strategies in post-fire environments (Cortini and Comeau, 2008). Recent developments in UAV technologies, including SfM photogrammetry, have promoted new opportunities for this purpose (Vanderwel et al., 2020). In this sense, the present study is pioneer in the use of UAV-MS and SfM photogrammetry as a proxy for evaluating intra and inter-specific plant competitive interactions in post-fire landscapes by means of a GEOBIA approach and machine learning algorithms. Competitive effects of understory shrub species were found to be largely accountable for spatial differences in growth among pine sapling individuals with distinct neighborhood conditions (Calama et al., 2019; Helluy et al., 2020).

4.1. Do the products derived from UAV data provide enough accuracy for species level classification and computation of structural information in recently burned landscapes?

Remote sensing techniques provide a means of scaling up vegetation measurements at species level from community to landscape scales (Anderson and Gaston, 2013; Fraser et al., 2016). However, the conventionally used remote sensing records for this purpose, such as multi-

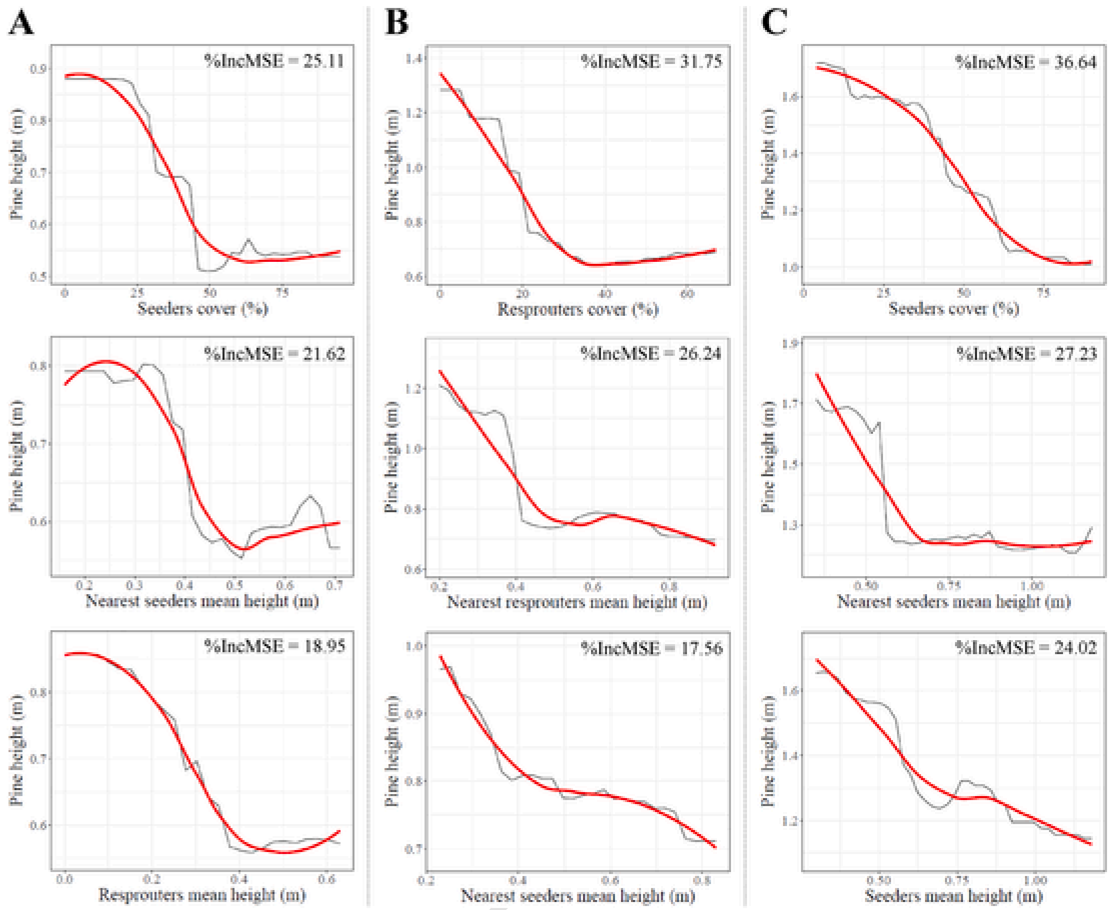

Fig. 4. Partial dependence plots showing the effects of competing vegetation on pine sapling growth and the relative importance of each predictor to the explained variance in parsimonious RF models (%IncMSE) for the Atlantic (A), Transition (B) and Mediterranean (C) sites. Red line represents a LOESS smooth curve. (For interpretation of the references to colour in this figure legend, the reader is referred to the Web version of this article.)

Table 7
Random Forest (RF) model accuracy results in the analysis of vegetation neighborhood competition on pine saplings.

Explained variance (R^2)	Atlantic site	Transition site	Mediterranean site
Parsimonious model	0.74	0.75	0.82
Full model	0.58	0.55	0.69

spectral imagery acquired from satellite and aerial sensor platforms (Xie et al., 2008), do not provide enough spatial resolution or structural information to characterize the variability in species composition and height, especially in burned areas with high shrub dominance and scattered tree saplings (Yang et al., 2012), as in our study sites. In addition, the typical relatively low point density of conventional LiDAR technology and its lack of spectral information would not allow to capture the fine-scale composition at species-level and the heterogeneity of the observed post-fire plant communities, as well as their structural characteristics (Fraser et al., 2016). In this sense, our results evidenced that the fusion of spectral and height information derived from SfM processing of UAV-borne data at very high spatial resolution was a sound alternative for mapping vegetation at species level in heterogeneous post-fire environments, as we initially hypothesized. The evaluated landscapes featured a fine-scale ground spatial variation arising from complex mixtures of plant species, soil types and burned legacies (Fernández-Guisuraga et al., 2019a), where shrub and sapling individuals jointly contribute to the majority of the leaf area and foliar biomass (Yang et al., 2012). Under such circumstances, very high spatial resolution data are critical to account for the fine-grained arrangement of vegetation in small patches (Fernández-Guisuraga et al., 2018, 2021b), particularly at the level of individual species (Sankey et al., 2017). Besides canopy height models, the inclusion of MS UAV data was mandatory to attain desirable outputs (OA = 83.67% ± 3.06%), in comparison with RGB spectral data (OA = 74.33% ± 3.21%) dealing with fine scale object-based image classification under high vegetation complexity. Likewise, PA and UA of each plant species were higher using MS-CHM (71%–96%) than RGB-CHM (58%–78%) as input data. In these scenarios, the higher spatial resolution of RGB sensors cannot overcome their lack of spectral information as compared to MS sensors (Komárek et al., 2018). For instance, the red edge band included in the Parrot Sequoia MS sensor features a high sensitivity to shifts in vegetation leaf biochemical and biophysical parameters (Fernández-Guisuraga et al., 2020a), as well as in canopy structure (Schumacher et al., 2016). Accordingly, this band provided valuable information for characterizing heterogeneous vegetation recovery patterns, as found in previous research (Fernández-Guisuraga et al., 2019b). Also, we evidenced that the parametrization of the MRS algorithm in the GEOBIA approach must carefully consider both the spatial resolution of the remote sensing data and the actual scale of the different vegetation land cover classes to prevent impacts on classification accuracy. The use of multilevel segmentation approaches considering several scales according to the variability in the patch size of the land covers of interest in burned landscapes is critical to minimize the under-segmentation likelihood and the production of mixed objects that could be misclassified because inconsistencies between their spectral characterization and their actual content (Radoux and Bogaert, 2014; Ma et al., 2015). Although this concern is particularly evident and unavoidable in areas with diffuse gradients between cover types, specially at UAV higher flight altitudes (Horning et al., 2020), the multilevel segmentation provided an unbiased identification and representation of each plant species in the output map, evidenced by the consistency between PA-UA of each class, despite their different actual scales, and OA (Ma et al., 2015; Prošek and Šímová, 2019) within the three sites using MS-CHM data as classification input.

Our results are in accordance with OA and PA-UA attained in previous research dealing with classification at species level through UAV multispectral and height data (Komárek et al., 2018; Prošek and Šímová, 2019). As evidenced by these authors, among others (Nevalainen et al., 2017; Sankey et al., 2017; Sothe et al., 2019), the spectral separability of the most frequent misclassified species in the present study (*Cytisus scoparius* and *Ulex europaeus* in the Atlantic site, and *Ulex parviflorus* and *Quercus coccifera* in the Mediterranean site) could have been further improved by using hyperspectral UAV-borne data due to the similar spectral response of these species at the four wavelengths in which Parrot Sequoia channels span. Likewise, the use of multi-temporal UAV data, or data fusion of dense time series satellite imagery and mono-temporal UAV orthoimagery (Gränzig et al., 2021), could have enhanced the spectral separability by capturing the heterogeneity in the phenology variations between species of the study sites, such as leaf emergence or flowering, as evidenced in several studies (e.g. Sheeren et al., 2016; Grabska et al., 2019; Gränzig et al., 2021). Additionally, the substantial height variability of some species in the study sites, such as *Quercus coccifera* individuals in the Mediterranean site, could be a potential explanation of some species misclassification. Under this situation, the CHM would not be meaningful as a classification input to characterize these species according to their height, relying exclusively on spectral information for this purpose (Prošek and Šímová, 2019).

The agreement between field measurements of vegetation cover and mean height, and those derived from the UAV classified map and the CHM, respectively, was markedly high ($R^2 > 0.86$ and RMSE $< 6.36\%$ and $R^2 > 0.70$ and RMSE < 28.24 cm), in line with previous studies with similar UAV imagery acquisition conditions (flight height above 90 m AGL and along-track/cross-track overlap higher than 75%) in heterogeneous shrublands (Fraser et al., 2016; Yang et al., 2021) and complex agricultural systems (Han et al., 2018). Overall, these findings supported the subsequent analyses of competition effects on pine saplings without misrepresented results (Schmidt et al., 2017).

4.2. Is the growth of pine saplings conditioned by intra and interspecific competitive effects?

During the first and second years after fire, pine seedling density often reaches its maximum value (Ne'eman et al., 1995) because of favorable microscale conditions (Moya et al., 2008) and increased incident solar radiation (Calvo et al., 2008). In such early, critical period, severe density-dependent effects of intra-specific competition can be expected on the survival and growth of *Pinus pinaster* and *Pinus halepensis* seedlings, as evidenced in numerous studies (e.g. Ne'eman et al., 1995; De las Heras et al., 2002; Calvo et al., 2008; Taboada et al., 2017). However, we have found no relevant intra-specific competitive effects on the relative growth in height of pine saplings four years after the fire, contrary to what we hypothesized. In this sense, De las Heras et al. (2002) detected detrimental intra-specific competition effects on pine saplings growth only up to the second post-fire year. This trend may be associated with the decline of pine sapling density because of the high mortality rates in the early post-fire period (Moravec, 1990) and, also, with a better mineral nutrition capacity during the first years of sapling growth (Ne'eman et al., 1992).

Four years after fire, as we expected, the relative growth in height of *Pinus pinaster* and *Pinus halepensis* saplings was impacted by inter-specific competitive effects of neighboring shrub species, the stronger the effect as the cover and height of such species increased. In this case, inter-specific competition is expected to occur until the young pine saplings clearly overtop the dominant tall shrub layer (Calvo et al., 2008; Zhang et al., 2020), on average between 10 and 15 years after fire (Moravec, 1990). In *Pinus pinaster* and *Pinus halepensis* ecosystems, belowground competition of pine saplings for water and nutrients is considered one of the main mechanisms of interaction with neighboring vegetation because of root interference (De las Heras et al., 2002; Sardans et al., 2004; Calvo et al., 2008; Rodríguez-García et al., 2011a). These interactions will be more intense with increasing space occupation (related to cover) and plant development (related to mean height) of shrub individuals in the sapling neighborhood, as evidenced in this study. In addition, *Pinus pinaster* and *Pinus halepensis* saplings feature strongly light-dependent growth patterns (Zavala et al., 2011), so asymmetric competition for light is also a frequent interaction in pine sapling neighborhoods (Calvo et al., 2008), particularly when the saplings are well-developed and have greater access to soil resources (Rodríguez-García et al., 2011a). Indeed, we found that light limitation because of neighbor shade had a major negative impact on pine sapling growth. The observed non-linear relationships between shrub structure variables and relative growth in height of pine saplings were also observed in planted saplings of ponderosa pine (*Pinus ponderosa* Dougl. ex Laws.) in Oregon and Montana (Wagner et al., 1989). These relationships enable the implementation of possible competing thresholds to the observed patterns.

Although it is well known that microscale conditions (e.g. topography, woody debris cover, humidity and their complex interactions) could affect pine forest regrowth (Rodríguez-García et al., 2011a; Taboada et al., 2017), we focused only on the measurement of neighboring effects on pine saplings growth (a manageable property) through UAV-based techniques to provide a decision-making tool in burned areas with high ground cover heterogeneity. Incorporating microscale variables into the RF models would likely improve their accuracy, but competitive effects alone significantly explained the growth of pine saplings in the three study sites ($R^2 > 0.74$), demonstrating their importance in the post-fire management of fire-prone pine ecosystems.

4.3. Do the shrub competitive effects differ according to their fire-adaptive traits and are these patterns maintained throughout different environmental conditions?

We found that competition intensity of seeders and resprouters shrubs varied along the Atlantic-Transition-Mediterranean gradient. In the Atlantic and Mediterranean sites, obligate seeder shrubs (*Ulex europaeus* and *Ulex parviflorus* and *Cistus* sp., respectively) were responsible for the strongest competitive effects on pine saplings growth. *Ulex* sp. and *Cistus* sp. have physically dormant seeds in the soil bank that massively germinate after fire, favored by the thermal shock (De las Heras et al., 2002; Baeza and Roy, 2008). The high density in the early post-fire stages of both genera, along with the presence of photosynthesizing stems in *Ulex* sp. confers a significant competitive advantage over other taxa in post-fire environments, where light and water are limiting factors (Baeza, 2001). In the Mediterranean site, the vigorous resprouter *Quercus coccifera* did not exhibit any relevant inter-specific effect, despite its high post-fire regeneration rate (Vilà and Terradas, 1995). Likewise, a moderate competitive interaction of resprouter shrubs was observed under Atlantic conditions on pine sapling growth, although these species, such as *Erica* sp., can readily recolonize the space occupied before the fire from surviving tissues and feature highly competitive abilities (Calvo et al., 2003; Taboada et al., 2017). Indeed, inter-specific competition interactions of resprouter shrubs (*Erica* sp. and *Pterospartum tridentatum*) were substantially more pronounced than those of seeders in the Transition site.

Partially contradictory results regarding this competition gradient were obtained based on the two most widely accepted ecological models which explain scale patterns of competition intensity of seeder and resprouter life history types. The gap-dependent model (Keeley and Zedler, 1978; Keeley et al., 2016) establishes that high intensities of seeder species competition are promoted in more open post-disturbance habitats against more densely vegetated areas, where resprouter species feature competitive advantages as they are assumed to be better competitors than seeders (Taboada et al., 2017). The Atlantic and Mediterranean sites exhibit a lower vegetation cover and fuel continuity than the Transition site in the first post-fire years (Fernández-Guisuraga et al., 2020b), as well as a high presence of bare soil and rock outcrops, which support the intense neighboring effects of seeder shrubs in these sites.

For its part, the resource-productivity model (Clarke et al., 2005) concludes that as resource availability increases (mainly moisture and nutrients) from lower to higher productivity environments, resprouting confers competitive advantages over seeding strategy (Pausas and Keeley, 2014). In this sense, the highest competition intensity would have been expected from resprouter shrubs in the moist and fertile Atlantic site (Fernández-García et al., 2020). Nevertheless, the effect of resprouter species was still evident at this site (19% versus 47% of RF model relative importance for the sum of resprouters and seeders included variables, respectively), and the balance of competition effects between both fire adaptive-traits was consistent with the resource-productivity model in the Transition and Mediterranean sites.

4.4. Management implications

There is growing concern for decision makers, forest stakeholders and citizens in general about the ecological and socio-economic impacts of stand-replacing wildfires on the regeneration of the dominant tree species in the Mediterranean Basin (Moreira et al., 2011; Raftoyannis et al., 2014), particularly under climate and land use/land cover changes (Fernandes, 2013; González-De Vega et al., 2016). These factors have promoted the expansion of shrub species prone to large, recurrent and severe wildfires (González-De Vega et al., 2016; Fernández-Guisuraga et al., 2021b), which have been shown to exert strong competitive effects on pine saplings' performance in the first years after the fire. The non-linear relationships evidenced in this study between the structure of neighboring shrubs and the growth of pine seedlings/saplings have profound implications for considering possible competing thresholds in post-fire decision-making processes. For instance, woody understory species cover higher than 30% and a height that allows to overtop saplings, was found to severely impact the saplings' growth, which is in line with the findings evidenced by McDonald and Fiddler (2011) in Ponderosa pine plantations in California. Under this situation, moderate mechanical treatments such as cutting can be effective in controlling woody competitors for ensuring the regeneration of the dominant tree species, either around pine saplings or in the form of area-wide treatments (Balandier et al., 2006; Lucas-Borja et al., 2016). These treatments yield less drastic changes to the structure of the shrub understory community than more intensive approaches such as herbicide application or root dislodging (Haeussler et al., 1999), while releasing the young pine saplings from light competition (Balandier et al., 2006). Other treatments such as long-lasting mulches in combination with moderate mechanical approaches for controlling unwanted vegetation have proven to be effective in enhancing Ponderosa pine saplings growth in the Sierra Nevada of California (McDonald et al., 1994). Nevertheless, the impact of the shrub management strategies on the ecosystem microclimate (Helluy et al., 2020; Prévosto et al., 2020) needs to be considered since it may lead to changes in composition and structure of the understory community, and, therefore, to the net vegetation competitive effect (Balandier et al., 2006).

5. Conclusions

This pioneer study evaluated the reliability of UAV-borne RGB and MS data, as well as SfM photogrammetry, as a tool for assessing intra and inter-specific competition of neighboring vegetation on pine saplings by means of a GEOBIA approach and RF algorithm in three post-fire landscapes located along a climatic gradient. Data fusion of UAV MS imagery and CHM computed from a photogrammetry workflow enhanced vegetation mapping at species level in heterogeneous burned landscapes, whereas RGB-CHM data fusion lacked enough spectral information for this purpose, despite its higher spatial resolution. Intra-specific competitive effects on pine saplings growth were not detected in the medium term after the wildfire. In contrast, pine saplings development was severely affected by inter-specific competition of neighboring shrub species. The non-linear relationships of the interactions would allow to consider competing thresholds that could be implemented in post-fire management decision-making. The competition intensity of shrub species varied according to seeding and resprouting fire-adaptive traits along the climatic gradient following a gap dependence model, in which high intensity competition by seeders is expected in more open post-disturbance habitats against more densely vegetated areas. The proposed approach constitutes a valuable post-fire management tool for measuring the effect of neighborhood competition on the performance of pine saplings.

Credit author statement

José Manuel Fernández-Guisuraga: Conceptualization, Methodology, Validation, Formal analysis, Investigation, Writing – original draft. **Leonor Calvo:** Conceptualization, Methodology, Investigation, Resources, Writing – review & editing, Project administration, Funding acquisition. **Susana Suárez-Seoane:** Conceptualization, Methodology, Investigation, Resources, Writing – review & editing, Project administration, Funding acquisition.

Uncited references

.

Declaration of competing interest

The authors declare that they have no known competing financial interests or personal relationships that could have appeared to influence the work reported in this paper.

Acknowledgements

This study was financially supported by the Spanish Ministry of Economy and Competitiveness, and the European Regional Development Fund (ERDF), in the framework of the GESFIRE (AGL2013-48189-C2-1-R) and FIRESEVES (AGL2017-86075-C2-1-R) projects; and by the Regional Government of Castilla and León in the framework of the FIRECYL (LE033U14), SEFIRECYL (LE001P17) and WUIFIRECYL (LE005P20) projects. J.M. Fernández-Guisuraga is supported by a predoctoral fellowship from the Spanish Ministry of Education (FPU16/03070).

Appendix A. Supplementary data

Supplementary data to this article can be found online at https://doi.org/10.1016/j.jenvman.2021.114373.

References

Agisoft, 2019. Agisoft Metashape User Manual, Professional Edition. Version 1.5. https://www.agisoft.com/pdf/metashape-pro_1_5_en.pdf. (Accessed 3 December 2020).

Anderson, K., Gaston, K.J., 2013. Lightweight unmanned aerial vehicles will revolutionize spatial ecology. Front. Ecol. Environ. 11, 138–146.

Arnan, X., Quevedo, L., Rodrigo, A., 2013. Forest fire occurrence increases the distribution of a scarce forest type in the Mediterranean Basin. Acta Oecol. 46, 39–47.

Assmann, J.J., Myers-Smith, I.H., Kerby, J.T., Cunliffe, A.M., Daskalova, G.N., 2020. Drone data reveal heterogeneity in tundra greenness and phenology not captured by satellites. Environ. Res. Lett. 15, 125002.

Baatz, M., Schäpe, A., 2000. Multiresolution segmentation: an optimization approach for high quality multi-scale image segmentation. In: Proceedings of the 12th Symposium for Applied Geographic Information Processing, Salzburg, Austria. pp. 12–23.
Baeza, M.J., 2001. Aspectos ecológicos y técnicas de control del combustible (roza y quema controlada) en matorrales con alto riesgo de incendio dominados por Ulex parviflorus (Pourr.) Thesis dissertation. University of Alicante, Spain.
Baeza, M.J., Roy, J., 2008. Germination of an obligate seeder (Ulex parviflorus) and consequences for wildfire management. For. Ecol. Manag. 256, 685–693.
Balandier, P., Collet, C., Miller, J.H., Reynolds, P.E., Zedaker, S.M., 2006. Designing forest vegetation management strategies based on the mechanisms and dynamics of crop tree competition by neighbouring vegetation. Forestry 79, 3–27.
Baxter, P.W.J., Hamilton, G., 2018. Learning to fly: integrating spatial ecology with unmanned aerial vehicle surveys. Ecosphere 9, e02194.
Belgiu, M., Csillik, O., 2018. Sentinel-2 cropland mapping using pixel-based and object-based time-weighted dynamic time warping analysis. Rem. Sens. Environ. 204, 509–523.
Blaschke, T., 2010. Object based image analysis for remote sensing. ISPRS J. Photogrammetry Remote Sens. 65, 2–16.
Breiman, L., 2001. Random forests. Mach. Learn. 45, 5–32.
Broncano, M.J., Retana, J., 2004. Topography and forest composition affecting the variability in fire severity and post-fire regeneration occurring after a large fire in the Mediterranean basin. Int. J. Wildland Fire 13, 209–216.
Calama, R., Conde, M., de-Dios-García, J., Madrigal, G., Vázquez-Piqué, J., Gordo, F.J., Pardos, M., 2019. Linking climate, annual growth and competition in a Mediterranean forest: Pinus pinea in the Spanish Northern Plateau. Agric. For. Meteorol. 264, 309–321.
Calvo, L., Santalla, S., Marcos, E., Valbuena, L., Tárrega, R., Luis, E., 2003. Regeneration after wildfire in one community dominated by obligate seeder Pinus pinaster and in another dominated by a typical resprouter Quercus pyrenaica. For. Ecol. Manag. 184, 209–223.
Calvo, L., Santalla, S., Valbuena, L., Marcos, E., Tárrega, R., Luis-Calabuig, E., 2008. Post-fire natural regeneration of a Pinus pinaster forest in NW Spain. Plant Ecol. 197, 81–90.
Calvo, L., Hernández, V., Valbuena, L., Taboada, A., 2016. Provenance and seed mass determine seed tolerance to high temperatures associated to forest fires in Pinus pinaster. Ann. For. Sci. 73, 381–391.
Carabassa, V., Montero, P., Crespo, M., Padró, J.C., Pons, X., Balagué, J., Brotons, L., Maria Alcañiz, J., 2020. Unmanned aerial system protocol for quarry restoration and mineral extraction monitoring. J. Environ. Manag. 270, 110717.
Chergui, B., Pleguezuelos, J.M., Fahd, S., Santos, X., 2020. Modelling functional response of reptiles to fire in two Mediterranean forest types. Sci. Total Environ. 732, 139205.
Clarke, P.J., Knox, J.E., Wills, K.E., Campbell, M., 2005. Landscape patterns of woody plant response to crown fire: disturbance and productivity influence sprouting ability. J. Ecol. 93, 544–555.
Colefax, A.P., Butcher, P.A., Kelaher, B.P., 2018. The potential for unmanned aerial vehicles (UAVs) to conduct marine fauna surveys in place of manned aircraft. ICES (Int. Counc. Explor. Sea) J. Mar. Sci. 75, 1–8.
Cortes, C., Vapnik, V., 1995. Support-vector networks. Mach. Learn. 20, 273–297.
Cortini, F., Comeau, P.G., 2008. Evaluation of competitive effects of green alder, willow and other tall shrubs on white spruce and lodgepole pine in Northern Alberta. For. Ecol. Manag. 255, 82–91.
Cruzan, M.B., Weinstein, B.G., Grasty, M.R., Kohrn, B.F., Hendrickson, E.C., Arredondo, T.M., Thompson, P.G., 2016. Small unmanned aerial vehicles (micro-UAVs, drones) in plant ecology. Applications in Plant Sciences 4, 1600041.
Cutler, D.R., Edwards, T.C., Beard, K.H., Cutler, A., Hess, K.T., Gibson, J., Lawler, J.J., 2007. Random forests for classification in ecology. Ecology 88, 2783–2792.
Dandois, J.P., Olano, M., Ellis, E.C., 2015. Optimal altitude, overlap, and weather conditions for computer vision UAV estimates of forest structure. Rem. Sens. 7, 13895–13920.
Daryaei, A., Sohrabi, H., Atzberger, C., Immitzer, M., 2020. Fine-scale detection of vegetation in semi-arid mountainous areas with focus on riparian landscapes using Sentinel-2 and UAV data. Comput. Electron. Agric. 177, 105686.
De las Heras, J., Martínez-Sánchez, J.J., González-Ochoa, A.I., Ferrandis, P., Herranz, J.M., 2002. Establishment of Pinus halepensis Mill. sapling following fire: effects of competition with shrub species. Acta Oecol. 23, 91–97.
de Oliveira, E.K.B., Rezende, A.V., Mazzei, L., Júnior, L.S.M., Castro, R.V.O., d'Oliveira, M.V.N., Barros, Q.S., 2021. Competition indices after reduced impact logging in the Brazilian Amazon. J. Environ. Manag. 281, 111898.
Deng, L., Mao, Z., Li, X., Hu, Z., Duan, F., Yan, Y., 2018. UAV-based multispectral remote sensing for precision agriculture: a comparison between different cameras. ISPRS J. Photogrammetry Remote Sens. 146, 124–136.
Drăguţ, L., Tiede, D., Levick, S., 2010. ESP: a tool to estimate scale parameters for multiresolution image segmentation of remotely sensed data. Int. J. Geogr. Inf. Sci. 24, 859–871.
Drăguţ, L., Csillik, O., Eisank, C., Tiede, D., 2014. Automated parameterisation for multi-scale image segmentation on multiple layers. ISPRS J. Photogrammetry Remote Sens. 88, 119–127.
Duro, D.C., Franklin, S.E., Dubé, M.G., 2012. A comparison of pixel-based and object-based image analysis with selected machine learning algorithms for the classification of agricultural landscapes using SPOT-5 HRG imagery. Rem. Sens. Environ. 118, 259–272.
Eshel, A., Henig-Sever, N., Ne'eman, G., 2000. Spatial variation of seedling distribution in an east Mediterranean pine woodland at the beginning of post-fire succession. Plant Ecol. 148, 175–182.
Fang, L., Crocker, E.V., Yang, J., Yan, Y., Yang, Y., Liu, Z., 2019. Competition and burn severity determine post-fire sapling recovery in a nationally protected boreal forest of China: an analysis from very high-resolution satellite imagery. Rem. Sens. 11, 603.
Fernandes, P.M., 2013. Fire-smart management of forest landscapes in the Mediterranean basin under global change. Landsc. Urban Plann. 110, 175–182.
Fernandes, P.M., Vega, J.A., Jiménez, E., Rigolot, E., 2008. Fire resistance of European pines. For. Ecol. Manag. 256, 246–255.
Fernandes, P., Máguas, C., Correia, O., 2017. Combined effects of climate, habitat, and disturbance on seedling establishment of Pinus pinaster and Eucalyptus globulus. Plant Ecol. 218, 501–515.
Fernández-García, V., Fulé, P.Z., Marcos, E., Calvo, L., 2019. The role of fire frequency and severity on the regeneration of Mediterranean serotinous pines under different environmental conditions. For. Ecol. Manag. 444, 59–68.
Fernández-García, V., Marcos, E., Fulé, P.Z., Reyes, O., Santana, V.M., Calvo, L., 2020. Fire regimes shape diversity and traits of vegetation under different climatic conditions. Sci. Total Environ. 716, 137137.
Fernández-Guisuraga, J.M., Sanz-Ablanedo, E., Suárez-Seoane, S., Calvo, L., 2018. Using unmanned aerial vehicles in postfire vegetation survey campaigns through large and heterogeneous areas: opportunities and challenges. Sensors 18, 586.
Fernández-Guisuraga, J.M., Calvo, L., Fernández-García, V., Marcos-Porras, E., Taboada, A., Suárez-Seoane, S., 2019a. Efficiency of remote sensing tools for post-fire management along a climatic gradient. For. Ecol. Manag. 433, 553–562.
Fernández-Guisuraga, J.M., Suárez-Seoane, S., Calvo, L., 2019b. Modeling Pinus pinaster forest structure after a large wildfire using remote sensing data at high spatial resolution. For. Ecol. Manag. 446, 257–271.
Fernández-Guisuraga, J.M., Calvo, L., Suárez-Seoane, S., 2020a. Comparison of pixel unmixing models in the evaluation of post-fire forest resilience based on temporal series of satellite imagery at moderate and very high spatial resolution. ISPRS J. Photogrammetry Remote Sens. 164, 217–228.
Fernández-Guisuraga, J.M., Suárez-Seoane, S., Calvo, L., 2021a. Radiative transfer modeling to measure fire impact and forest engineering resilience at short-term. ISPRS J. Photogrammetry Remote Sens. 176, 30–41.
Fernández-Guisuraga, J.M., Verrelst, J., Calvo, L., Suárez-Seoane, S., 2021b. Hybrid inversion of radiative transfer models based on high spatial resolution satellite reflectance data improves fractional vegetation cover retrieval in heterogeneous ecological systems after fire. Rem. Sens. Environ. 255, 112304.
Fernández-Guisuraga, J.M., Suárez-Seoane, S., Calvo, L., 2020b. Transferability of vegetation recovery models based on remote sensing across different fire regimes. Applied Vegeteation Science 23, 441–451.
Fraser, R.H., Olthof, I., Lantz, T.C., Schmitt, C., 2016. UAV photogrammetry for mapping vegetation in the low-Arctic. Arctic Science 2, 79–102.
García-Llamas, P., Suárez-Seoane, S., Fernández-Manso, A., Quintano, C., Calvo, L., 2020. Evaluation of fire severity in fire prone-ecosystems of Spain under two different environmental conditions. J. Environ. Manag. 271, 110706.
Getzin, S., Nuske, R.S., Wiegand, K., 2014. Using unmanned aerial vehicles (UAV) to quantify spatial gap patterns in forests. Rem. Sens. 6, 6988–7004.
González-De Vega, S., De las Heras, J., Moya, D., 2016. Resilience of Mediterranean terrestrial ecosystems and fire severity in semiarid areas: responses of Aleppo pine forests in the short, mid and long term. Sci. Total Environ. 573, 1171–1177.
Grabska, E., Hostert, P., Pflugmacher, D., Ostapowicz, K., 2019. Forest stand species mapping using the sentinel-2 time series. Rem. Sens. 11, 1197.
Gränzig, T., Fassnacht, F.E., Kleinschmit, B., Förster, M., 2021. Mapping the fractional coverage of the invasive shrub Ulex europaeus with multi-temporal Sentinel-2 imagery utilizing UAV orthoimages and a new spatial optimization approach. Int. J. Appl. Earth Obs. Geoinf. 96, 102281.
Haeussler, S., Bedfor, L., Boateng, J.O., MacKinnon, A., 1999. Plant community responses to mechanical site preparation in northern interior British Columbia. Can. J. For. Res. 29, 1084–1100.
Han, X., Thomasson, J.A., Bagnall, G.C., Pugh, N.A., Horne, D.W., Rooney, W.L., Jung, J., Chang, A., Malambo, L., Popescu, S.C., Gates, I.T., Cope, D.A., 2018. Measurement and calibration of plant-height from fixed-wing UAV images. Sensors 18, 4092.
Haralick, R.M., Shanmugam, K., Dinstein, I.H., 1973. Textural features for image classification. IEEE Transactions on Systems, Man, and Cybernetics 3, 610–621.
Healey, S.P., Yang, Z., Gorelick, N., Ilyushchenko, S., 2020. Highly local model calibration with a new GEDI LiDAR asset on google earth engine reduces landsat forest height signal saturation. Rem. Sens. 12, 2840.
Helluy, M., Prévosto, B., Cailleret, M., Fernandez, C., Balandier, P., 2020. Competition and water stress indices as predictors of Pinus halepensis Mill. radial growth under drought. For. Ecol. Manag. 460, 117877.
Horning, N., Fleishman, E., Ersts, P.J., Fogarty, F.A., Wohlfeil Zillig, M., 2020. Mapping of land cover with open-source software and ultra-high-resolution imagery acquired with unmanned aerial vehicles. Remote Sensing in Ecology and Conservation 6, 487–497.
Jones, A., Montanarella, L., Jones, R., 2005. Soil Atlas of Europe. European Commission.
Kane, V.R., Cansler, C.A., Povak, N.A., Kane, J.T., McGaughey, R.J., Lutz, J.A., Churchill, D.J., North, M.P., 2015. Mixed severity fire effects within the Rim fire: relative importance of local climate, fire weather, topography, and forest structure. For. Ecol. Manag. 358, 62–79.
Keeley, J.E., Pausas, J.G., 2019. Distinguishing disturbance from perturbations in fire-prone ecosystems. Int. J. Wildland Fire 28, 282–287.
Keeley, J.E., Zedler, P.H., 1978. Reproduction of chaparral shrubs after fire: a comparison of the sprouting and seeding strategies. Am. Midl. Nat. 99, 141–162.
Keeley, J.E., Pausas, J.G., Rundel, P.W., Bond, W.J., Bradstock, R.A., 2011. Fire as an evolutionary pressure shaping plant traits. Trends Plant Sci. 16, 406–411.
Keeley, J.E., Bond, W.J., Bradstock, R.A., Pausas, J.G., Rundel, P.W., 2012. Fire in Mediterranean Climate Ecosystems: Ecology, Evolution and Management. Cambridge University Press, Cambridge, United Kingdom.
Keeley, J.E., Thomas Parker, V., Vasey, M.C., 2016. Resprouting and seeding hypotheses:

a test of the gap-dependent model using resprouting and obligate seeding subspecies of Arctostaphylos. Plant Ecol. 217, 743–750.
Knapp, B.O., Wang, G.G., Walker, J.L., 2008. Relating the survival and growth of planted longleaf pine seedlings to microsite conditions altered by site preparation treatments. For. Ecol. Manag. 255, 3768–3777.
Komárek, J., Klouček, T., Prošek, J., 2018. The potential of Unmanned Aerial Systems: a tool towards precision classification of hard-to-distinguish vegetation types? Int. J. Appl. Earth Obs. Geoinf. 71, 9–19.
Lanzer, N.B., Lee, T.D., Ducey, M.J., Eisenhaure, S.E., 2017. Sapling white pine (Pinus strobus L.) exhibits growth response following selective release from competition with glossy buckthorn (Frangula alnus P. Mill) and associated vegetation. For. Ecol. Manag. 404, 280–288.
Li, M., Ma, L., Blaschke, T., Cheng, L., Tiede, D., 2016. A systematic comparison of different object-based classification techniques using high spatial resolution imagery in agricultural environments. Int. J. Appl. Earth Obs. Geoinf. 49, 87–98.
Liang, W., Abidi, M., Carrasco, L., McNelis, J., Tran, L., Li, Y., Grant, J., 2020. Mapping vegetation at species level with high-resolution multispectral and lidar data over a large spatial area: a case study with kudzu. Rem. Sens. 12, 609.
Liaw, A., Wiener, M., 2002. Classification and regression by RandomForest. R. News 2, 18–22.
Liu, Y., Biana, L., Menga, Y., Wanga, H., Zhanga, S., Yanga, Y., Shaoa, X., Wang, B., 2012. Discrepancy measures for selecting optimal combination of parameter values in object-based image analysis. ISPRS J. Photogrammetry Remote Sens. 68, 144–156.
Liu, J., Li, P., Wang, X., 2015. A new segmentation method for very high resolution imagery using spectral and morphological information. ISPRS J. Photogrammetry Remote Sens. 101, 145–162.
Lo, C., Lin, C., 2013. Growth-competition-based stem diameter and volume modeling for tree-level forest inventory using airborne LiDAR data. IEEE Trans. Geosci. Rem. Sens. 51, 2216–2226.
Lourenço, P., Teodoro, A.C., Gonçalves, J.A., Honrado, J.P., Cunha, M., Sillero, N., 2021. Assessing the performance of different OBIA software approaches for mapping invasive alien plants along roads with remote sensing data. Int. J. Appl. Earth Obs. Geoinf. 95, 102263.
Lucas-Borja, M.E., Candel-Pérez, D., García Morote, F.A., Onkelinx, T., Tíscar, P.A., Balandier, P., 2016. Pinus nigra Arn. ssp. salzmannii seedling recruitment is affected by stand basal area, shrub cover and climate interactions. Ann. For. Sci. 73, 649–656.
Ma, L., Cheng, L., Li, M., Liu, Y., Ma, X., 2015. Training set size, scale, and features in Geographic Object-Based Image Analysis of very high resolution unmanned aerial vehicle imagery. ISPRS J. Photogrammetry Remote Sens. 102, 14–27.
Ma, Q., Su, Y., Tao, S., Guo, Q., 2017. Quantifying individual tree growth and tree competition using bi-temporal airborne laser scanning data: a case study in the Sierra Nevada Mountains, California. International Journal of Digital Earth 11, 485–503.
Maia, P., Pausas, J.G., Vasques, A., Keizer, J.J., 2012. Fire severity as a key factor in post-fire regeneration of Pinus pinaster (Ait.) in Central Portugal. Ann. For. Sci. 69, 489–498.
Martin-Ducup, O., Schneider, R., Fournier, R.A., 2016. Response of sugar maple (acer saccharum, marsh.) tree crown structure to competition in pure versus mixed stands. For. Ecol. Manag. 374, 20–32.
Matese, A., Toscano, P., Di Gennaro, S.F., Genesio, L., Vaccari, F.P., Primicerio, J., Belli, C., Zaldei, A., Bianconi, R., Gioli, B., 2015. Intercomparison of UAV, aircraft and satellite remote sensing platforms for precision viticulture. Rem. Sens. 7, 2971–2990.
McDonald, P.M., Fiddler, G.O., 2011. Twenty-five Years of Managing Vegetation in Conifer Plantations in Northern and Central California: Results, Application, Principles, and Challenges. USDA, For. Serv General Technical Report PSW-GTR-231, Pacific Southwest Research Station.
McDonald, P.M., Fiddler, G.O., Henry, W.T., 1994. Large mulches and manual release enhance growth of ponderosa pine seedlings. N. For. 8, 169–178.
Metz, J., Seidel, D., Schall, P., Scheffer, D., Schulze, E.-D., Ammer, C., 2013. Crown modeling by terrestrial laser scanning as an approach to assess the effect of aboveground intra- and interspecific competition on tree growth. For. Ecol. Manag. 310, 275–288.
Modica, G., Messina, G., De Luca, G., Fiozzo, V., Praticò, S., 2020. Monitoring the vegetation vigor in heterogeneous citrus and olive orchards. A multiscale object-based approach to extract trees' crowns from UAV multispectral imagery. Comput. Electron. Agric. 175, 105500.
Moravec, J., 1990. Regeneration of N.W. Africa Pinus halepensis forests following fire. Vegetatio 87, 29–36.
Moreira, F., Viedma, O., Arianoutsou, M., Curt, T., Koutsias, N., Rigolot, E., Barbati, A., Corona, P., Vaz, P., Xanthopoulos, G., Mouillot, F., Bilgili, E., 2011. Landscape-wildfire interactions in southern Europe: implications for landscape management. J. Environ. Manag. 92, 2389–2402.
Mountrakis, G., Im, J., Ogole, C., 2011. Support vector machines in remote sensing: a review. ISPRS J. Photogrammetry Remote Sens. 66, 247–259.
Moya, D., De las Heras, J., López-Serrano, F.R., Leone, V., 2008. Optimal intensity and age of management in young Aleppo pine stands for post-fire resilience. For. Ecol. Manag. 255, 3270–3280.
Moya, D., González-De-Vega, S., García-Orenes, F., Morugán-Coronado, A., Arancegui, V., Mataix-Solera, J., Lucas-Borja, M.E., De las Heras, J., 2018. Temporal characterisation of soil-plant natural recovery related to fire severity in burned Pinus halepensis Mill. Forests. Sci. Total Environ. 640–641, 42–51.
Moya, D., González-De Vega, S., Lozano, E., García-Orenes, F., Mataix-Solera, J., Lucas-Borja, M.E., de las Heras, J., 2019. The burn severity and plant recovery relationship affect the biological and chemical soil properties of Pinus halepensis Mill. stands in the short and mid-terms after wildfire. J. Environ. Manag. 235, 250–256.
Moya, D., Fonturbel, M.T., Lucas-Borja, M.E., Peña, E., Alfaro-Sanchez, R., Plaza-Álvarez, P.A., González-Romero, J., de Las Heras, J., 2021. Burning season and vegetation coverage influenced the community-level physiological profile of Mediterranean mixed-mesogean pine forest soils. J. Environ. Manag. 277, 111405.
Müllerová, J., Brůna, J., Bartaloš, T., Dvořák, P., Vítková, M., Pyšek, P., 2017. Timing Is important: unmanned aircraft vs. Satellite imagery in plant invasion monitoring. Front. Plant Sci. 8, 1–13.
Myint, S.W., Gober, P., Brazel, A., Grossman-Clarke, S., Weng, Q., 2011. Per-pixel vs. object-based classification of urban land cover extraction using high spatial resolution imagery. Rem. Sens. Environ. 115, 1145–1161.
Ne'eman, G.H., Lahav, H., Izhaki, I., 1992. Spatial pattern of seedlings one year after fire in a Mediterranean pine forest. Oecologia 91, 365–370.
Ne'eman, G.H., Lahav, H., Izhaki, I., 1995. Recovery of vegetation in a natural east Mediterranean pine forest on Mount Carmel, Israel, as affected by management strategies. For. Ecol. Manag. 75, 17–26.
Nevalainen, O., Honkavaara, E., Tuominen, S., Viljanen, N., Hakala, T., Yu, X., Hyyppä, J., Saari, H., Pölönen, I., Imai, N.N., Tommaselli, A.M.G., 2017. Individual tree detection and classification with UAV-based photogrammetric point clouds and hyperspectral imaging. Rem. Sens. 9, 185.
Ninyerola, M., Pons, X., Roure, J.M., 2005. Atlas Climático Digital de la Península Ibérica. Metodología y aplicaciones en bioclimatología y geobotánica. Universidad Autónoma de Barcelona.
Nuijten, R.J.G., Kooistra, L., De Deyn, G.B., 2019. Using unmanned aerial systems (UAS) and object-based image analysis (OBIA) for measuring plant-soil feedback effects on crop productivity. Drones 3, 54.
Oliveira, S., Oehler, F., San-Miguel-Ayanz, J., Camia, A., Pereira, M.C., 2012. Modeling spatial patterns of fire occurrence in mediterranean europe using multiple regression and random forest. For. Ecol. Manag. 275, 117–129.
O'Brien, M.J., O'Hara, K.L., Erbilgin, N., Wood, D.L., 2007. Overstory and shrub effects on natural regeneration processes in native Pinus radiata stands. For. Ecol. Manag. 240, 178–185.
Parker, W.C., Pitt, D.G., Morneault, A.E., 2010. Influence of woody and herbaceous vegetation control on leaf gas exchange, water status, and nutrient relations of eastern white pine (Pinus strobus L.) seedlings planted in a central Ontario clearcut. For. Ecol. Manag. 260, 2012–2022.
Parrot, 2020. Parrot Sequoia Support. https://community.parrot.com/t5/Sequoia/bd-p/Sequoia. (Accessed 3 December 2020).
Pausas, J.G., 2004. Changes in fire and climate in the eastern iberian Peninsula (Mediterranean Basin). Clim. Change 63, 337–350.
Pausas, J.G., Keeley, J.E., 2014. Evolutionary ecology of resprouting and seeding in fire-prone ecosystems. New Phytol. 204, 55–65.
Pausas, J.G., Llovet, J., Rodrigo, A., Vallejo, R., 2008. Are wildfires a disaster in the Mediterranean basin? A review. Int. J. Wildland Fire 17, 713–723.
Prévosto, B., Helluy, M., Gavinet, J., Fernandez, C., Balandier, P., 2020. Microclimate in Mediterranean pine forests: what is the influence of the shrub layer? Agric. For. Meteorol. 282, 107856.
Probst, P., Boulesteix, A.L., 2018. To tune or not to tune the number of trees in Random Forest. J. Mach. Learn. Res. 18, 1–18.
Prošek, J., Šímová, P., 2019. UAV for mapping shrubland vegetation: does fusion of spectral and vertical information derived from a single sensor increase the classification accuracy? Int. J. Appl. Earth Obs. Geoinf. 75, 151–162.
R Core Team, 2020. R: A Language and Environment for Statistical Computing. R Foundation for Statistical Computing, Vienna, Austria. https://www.R-project.org/.
Radoux, J., Bogaert, P., 2014. Accounting for the area of polygon sampling units for the prediction of primary accuracy assessment indices. Rem. Sens. Environ. 142, 9–19.
Raftoyannis, Y., Nocentini, S., Marchi, E., Calama-Sainz, R., Garcia-Guemes, C., Pilas, I., Peric, S., Amaral-Paulo, J., Moreira-Marcelino, A.C., Costa-Ferreira, M., Kakouris, E., Lindner, M., 2014. Perceptions of forest experts on climate change and fire management in European Mediterranean forests. iForest 7, 33–41.
Richardson, D.M., 2000. Ecology and Biogeography of Pinus. Cambridge University Press, Cambridge, United Kingdom.
Rodríguez-García, E., Ordóñez, C., Bravo, F., 2011a. Effects of shrub and canopy cover on the relative growth rate of Pinus pinaster Ait. seedlings of different sizes. Ann. For. Sci. 68, 337–346.
Rodríguez-García, E., Bravo, F., Spies, T.A., 2011b. Effects of overstorey canopy, plant–plant interactions and soil properties on Mediterranean maritime pine seedling dynamics. For. Ecol. Manag. 262, 244–251.
Sagra, J., Ferrandis, P., Plaza-Álvarez, P.A., Lucas-Borja, M.E., González-Romero, J., Alfaro-Sánchez, R., De las Heras, J., Moya, D., 2018. Regeneration of Pinus pinaster Aiton after prescribed fires: response to burn timing and biogeographical seed provenance across a climatic gradient. Sci. Total Environ. 637, 1550–1558.
Sánchez-Pinillos, M., Ameztegui, A., Kitzberger, T., Coll, L., 2018. Relative size to resprouters determines post-fire recruitment of non-serotinous pines. For. Ecol. Manag. 429, 300–307.
Sankey, T., Donager, J., McVay, J., Sankey, J.B., 2017. UAV lidar and hyperspectral fusion for forest monitoring in the southwestern USA. Rem. Sens. Environ. 195, 30–43.
Sardans, J., Rodà, F., Peñuelas, J., 2004. Phosphorus limitation and competitive capacities of Pinus halepensis and Quercus ilex subsp. rotundifolia on different soils. Plant Ecol. 174, 307.
Schmidt, J., Fassnacht, F.E., Neff, C., Lausch, A., Kleinschmit, B., Förster, M., Schmidtlein, S., 2017. Adapting a Natura 2000 field guideline for a remote sensing-based assessment of heathland conservation status. Int. J. Appl. Earth Obs. Geoinf. 60, 61–71.
Schumacher, P., Mislimshoeva, B., Brenning, A., Zandler, H., Brandt, M., Samimi, C., Koellner, T., 2016. Do red edge and texture attributes from high-resolution satellite data improve wood volume estimation in a semi-arid mountainous region? Rem. Sens. 8, 540.
Seidl, R., Rammer, W., Spies, T.A., 2014. Disturbance legacies increase the resilience of

forest ecosystem structure, composition, and functioning. Ecol. Appl. 24, 2063–2077.
Sheeren, D., Fauvel, M., Josipovi´c, V., Lopes, M., Planque, C., Willm, J., Dejoux, J.-F., 2016. Tree species classification in temperate forests using formosat-2 satellite image time series. Rem. Sens. 8, 734.
Smith, A., 2010. Image segmentation scale parameter optimization and land cover classification using the Random Forest algorithm. Spatial Sci. 55, 69–79.
Smith, G.M., Morton, R.D., 2010. Real world objects in GEOBIA through the exploitation of existing digital cartography and image segmentation. Photogramm. Eng. Rem. Sens. 76, 163–171.
Sothe, C., Dalponte, M., Almeida, C.M.d., Schimalski, M.B., Lima, C.L., Liesenberg, V., Miyoshi, G.T., Tommaselli, A.M.G., 2019. Tree species classification in a highly diverse subtropical forest integrating UAV-based photogrammetric point cloud and hyperspectral data. Rem. Sens. 11, 1338.
Taboada, A., Tárrega, R., Marcos, E., Valbuena, L., Suárez-Seoane, S., Calvo, L., 2017. Fire recurrence and emergency post-fire management influence seedling recruitment and growth by altering plant interactions in fire-prone ecosystems. For. Ecol. Manag. 402, 63–75.
Tapias, R., Gil, L., Fuentes-Utrilla, P., Pardos, J.A., 2001. Canopy seed banks in Mediterranean pines of southeastern Spain: a comparison between Pinus halepensis Mill., Pinus pinaster Ait., Pinus nigra Arn. and Pinus pinea L. J. Ecol. 89, 629–638.
Tapias, R., Climent, J., Pardos, J.A., Gil, L., 2004. Life histories of Mediterranean pines. Plant Ecol. 171, 53–68.
Turetsky, M.R., Baltzer, J.L., Johnstone, J.F., Mack, M.C., McCann, K., Schuur, E.A.G., 2017. Losing legacies, ecological release, and transient responses: key challenges for the future of northern ecosystem science. Ecosystems 20, 23–30.
Turner, D., Lucieer, A., Watson, C.S., 2011. Development of an Unmanned Aerial Vehicle (UAV) for hyper-resolution vineyard mapping based on visible, multispectral and thermal imagery. In: Proceedings of the 34th International Symposium on Remote Sensing of Environment. Sydney, Australia.
Vanderwel, M.C., Lopez, E.L., Sprott, A.H., Khayyatkhoshnevis, P., Shovon, T.A., 2020. Using aerial canopy data from UAVs to measure the effects of neighbourhood competition on individual tree growth. For. Ecol. Manag. 461, 117949.
Vasantha, V.K., Keesara, V.R., 2020. Comparative study on crop type classification using support vector machine on UAV imagery. In: Jain, K., Khoshelham, K., Zhu, X., Tiwari, A. (Eds.), Proceedings of UASG 2019. Springer, Cham, Germany.
Vaz, P.G., Bugalho, M.N., Fedriani, J.M., Branco, M., Lecomte, X., Nogueira, C., Caldeira, M.C., 2019. Unravelling associations between tree-seedling performance, herbivory, competition, and facilitation in high nature value farmlands. J. Environ. Manag. 232, 1066–1074.
Versace, S., Gianelle, D., Frizzera, L., Tognetti, R., Garfì, V., Dalponte, M., 2019a.
Versace, S., Gianelle, D., Frizzera, L., Tognetti, R., Garfì, V., Dalponte, M., 2019b. Prediction of competition indices in a Norway spruce and silver fir-dominated forest using lidar data. Rem. Sens. 11, 2734.
Vilà, M., Terradas, J., 1995. Effects of competition and disturbance on the resprouting performance of the Mediterranean shrub Erica multiflora l. (Ericaceae). Am. J. Bot. 82, 1241–1248.
Vilà-Cabrera, A., Coll, L., Martínez-Vilalta, J., Retana, J., 2018. Forest management for adaptation to climate change in the Mediterranean basin: a synthesis of evidence. For. Ecol. Manag. 407, 16–22.
Vivian, L.M., Cary, G.J., 2012. Relationship between leaf traits and fire-response strategies in shrub species of a mountainous region of south-eastern Australia. Ann. Bot. 109, 197–208.
Wagner, R.G., Petersen, T.D., Ross, D.W., Radosevich, S.R., 1989. Competition thresholds for the survival and growth of ponderosa pine seedlings associated with woody and herbaceous vegetation. N. For. 3, 151–170.
Walker, R.B., Coop, J.D., Downing, W.M., Krawchuk, M.A., Malone, S.L., Meigs, G.W., 2019. How much forest persists through fire? High-resolution mapping of tree cover to characterize the abundance and spatial pattern of fire refugia across mosaics of burn severity. Forests 10, 782.
Wallace, L., Lucieer, A., Malenovský, Z., Turner, D., Vopěnka, P., 2016. Assessment of forest structure using two UAV techniques: a comparison of airborne laser scanning and structure from motion (SfM) point clouds. Forests 7, 62.
Watts, A.C., Perry, J.H., Smith, S.E., Burgess, M.A., Wilkinson, B.E., Szantoi, Z., Ifju, P.G., Percival, H.F., 2010. Small unmanned aircraft systems for low-altitude aerial surveys. J. Wildl. Manag. 74, 1614–1619.
Whitehead, K., Hugenholtz, C.H., 2014. Remote sensing of the environment with small unmanned aircraft systems (UASs), part 1: a review of progress and challenges. J. Unmanned Veh. Syst. 2, 69–85.
Whiteside, T.G., Boggs, G.S., Maier, S.F., 2011. Comparing object-based and pixel-based classifications for mapping savannas. Int. J. Appl. Earth Obs. Geoinf. 13, 884–893.
Witharana, C., Civco, D.L., 2014. Optimizing multi-resolution segmentation scale using empirical methods: exploring the sensitivity of the supervised discrepancy measure Euclidean distance 2 (ED2). ISPRS J. Photogrammetry Remote Sens. 87, 108–121.
Xie, Y., Sha, Z., Yu, M., 2008. Remote sensing imagery in vegetation mapping: a review. J. Plant Ecol. 1, 9–23.
Yang, X., 2011. Parameterizing support vector machines for land cover classification. Photogramm. Eng. Rem. Sens. 1, 27–37.
Yang, J., Weisberg, P.J., Bristow, N.A., 2012. Landsat remote sensing approaches for monitoring long-term tree cover dynamics in semi-arid woodlands: comparison of vegetation indices and spectral mixture analysis. Rem. Sens. Environ. 119, 62–71.
Yang, D., Morrison, B.D., Hantson, W., Breen, A.L., McMahon, A., Li, Q., Salmon, V.G., Hayes, D.J., Serbin, S.P., 2021. Landscape-scale characterization of Arctic tundra vegetation composition, structure, and function with a multi-sensor unoccupied aerial system. Environ. Res. Lett. 16, 085005.
Zavala, M.A., Espelta, J.M., Caspersen, J., Retana, J., 2011. Interspecific differences in sapling performance with respect to light and aridity gradients in Mediterranean pine–oak forests: implications for species coexistence. Can. J. For. Res. 41, 1432–1444.
Zhang, H., Fritts, J., Goldman, S., 2008. Image segmentation evaluation: a survey of unsupervised methods. Comput. Vis. Image Understand. 110, 260–280.
Zhang, J., Busse, M.D., Fiddler, G.O., Fredrickson, E., 2020. Thirteen-year growth response of ponderosa pine plantations to dominant shrubs (Arctostaphylos and Ceanothus). J. For. Res. 31, 1445–1451.
Zhao, D., Borders, B., Wilson, M., Rathbun, S.L., 2006. Modeling neighborhood effects on the growth and survival of individual trees in a natural temperate species-rich forest. Ecol. Model. 196, 90–102.